Table 5 Significantly enriched pathways from the microarray data

Pathway	Enrichment factor	P-value
CENP-A NAC-CAD complex (MIPS)	16.2	<0.001
PLK1 pathway (PID)	6.85	<0.001
Asthma (KEGG)	12.1	0.002
Cell adhesion molecules (KEGG)	3.53	0.002
Viral myocarditis (KEGG)	4.31	0.003
Allograft rejection (KEGG)	5.94	0.004
Mitotic prometaphase (Reactome)	3.66	0.006
Autoimmune thyroid disease (KEGG)	5.40	0.006
Graft versus host disease (KEGG)	5.40	0.006
GA13_PATHWAY (STKE)	5.24	0.007
Antigen processing and presentation (KEGG)	3.98	0.008
Type I Diabetes Mellitus (KEGG)	4.95	0.008

Contributors for curation: KEGG, KEGG: Kyoto Encyclopedia of Genes and Genomes; MIPS, MIPS database from CORUM (the Comprehensive Resource of Mammalian protein complexes); PID, Pathway Interaction Database (National Cancer Institute and Nature Publishing Group); STKE, Signal Transduction Knowledge Environment.

acetate and lead citrate (Figure 4A, insert), indicating that the particles were mineral particles rather than endogenous biomolecules. The diameter of the particles deposited in the lung was mostly within the range of 100–200 nm (Figure 4B, insert), and dissolving particles with approximately 20–60 nm diameter were also found in intracellular vesicles in the macrophage (Figure 4A, insert). The number of F4/80 positive cells (macrophages) did not significantly differ between ultrapure water and high-silica water groups by 14-day inhalation of the particles (Figure 4C - E). Abnormal macrophage accumulation was not observed in the lung of treated group. Although the total number of BALF cells was not affected by inhalation of particles from the humidifier with high-silica water (data not shown), the ratio of mononuclear cells in BALF tended to be increased (P =0.08) by 14-day inhalation of the particles (Figure 4F).

Discussion

Tap water contains dissolved solid composed of calcium, sodium, other minerals and anions. The secondary water quality standard of total dissolved solids (TDS) is established as 500 mg/L by the Ministry of Health, Labour and Welfare (Japan) and the Environmental Protection Agency (US). Water also has 'hardness', which is definable as the concentration of resistant solid matter determined as the equivalent concentration of calcium carbonate. Since the concentration and size distribution of particles from ultrasonic humidifier were well correlated with the concentration of minerals, they can be estimated by the TDS and hardness of water provided to the humidifier.

Humidifiers are usually operated with tap water, and in these experiments we found that operation with tap water generated submicron-sized particles (100–1000 μm), which contribute to the mass concentration, and that the humidifier released them into the air. In contrast, the particles from the humidifier operated with water containing a low concentration of minerals (4 mg/L Na or Ca) were mostly nano-sized (<100 nm); therefore they had only a small mass (<0.03 mg/m^3) but a large number concentration (>2 × 10^4/cm^3). This is the first study showing the characteristics of particles from the humidifier with tap water as well as other water with a low concentration of minerals. In the study using a series of calcium chloride solutions, the mass and the number concentrations were not well correlated. We concluded the cause of this worse correlation was another correlation between the mineral concentration of water and the particle size; i.e., the size was larger when the humidifier was operated with a water with higher concentration of minerals. Our data for the concentration of particles from ultrasonic humidifiers were measured in an experimental chamber (0.765 m^3, ventilation ratio 11.5 m^3/hr), whereas 0.59 mg/m^3, which

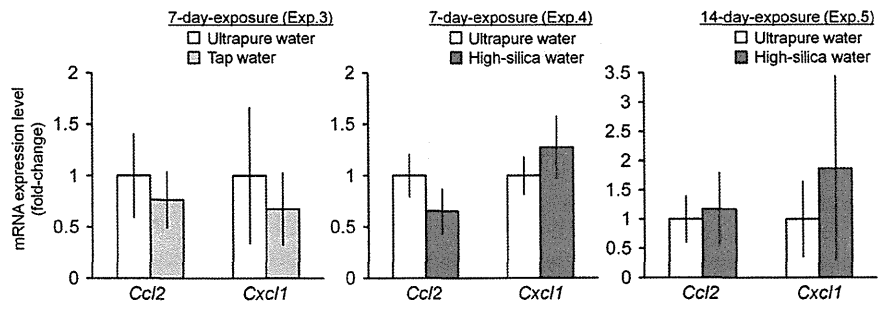

Figure 3 Effect of inhalation of particles released from ultrasonic humidifier on mRNA expression of *Ccl2*, and *Cxcl1* in the lung. Expression levels of *Ccl2* and *Cxcl1* in the lung tissues (Experiments 3–5, Table 1) were analyzed by an Mx3000P (Agilent Technologies) with SYBR Green Realtime PCR Master Mix (Toyobo). Relative expression levels of the target genes were calculated for each sample after normalization against *Gapdh*. Statistical analysis was performed using an unpaired *t*-test and the level of significance was set at P < 0.05.

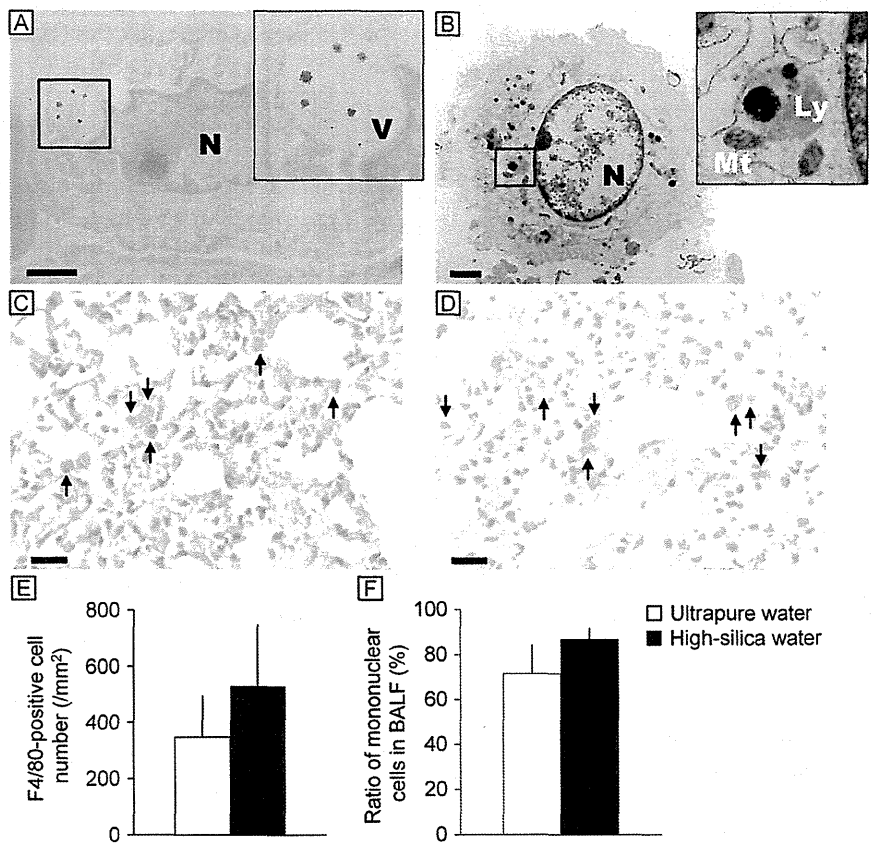

Figure 4 Images of electron microscopy and immunohistochemistry of cells in the lung tissue and bronchoalveolar lavage fluid. Transmission electron microscope images of macrophages in **(A)** lung tissue and **(B)** bronchoalveolar lavage fluid (BALF) of mouse of the 14-day high-silica water group (Experiment 5) are shown. The cells contained particle-like substances. Immunohistochemical F4/80 images of the lung tissue of **(C)** the ultrapure water group (control) and **(D)** the high-silica water group (14-day exposure, Experiment 5) are also shown. Arrows indicate F4/80 positive cells (macrophages). Mean number of F4/80-positive cells (±SD) is shown in **(E)**. There was no significant difference in the number of F4/80-positive cells in the lung between the ultrapure water and the high-silica water groups. **(F)** Ratio of mononuclear cells in BALF from Experiment 5 (14-day inhalation; $n = 4$/group). Scale bars represent **(A, B)** 1 μm and **(C, D)** 20 μm. Abbreviation: Ly, lysosome; Mt, mitochondria; N, nucleus; V, cytoplasmic vesicle.

is much greater than daily $PM_{2.5}$ standard (35 $\mu g/m^3$), was also reported when the humidifier was operated in an actual residence environment with tap water containing 303 mg/L TDS [14].

The health effect of airborne particles is one of the main issues in environmental toxicology. The size distribution data on the fog also indicated that it substantially contained submicron-sized particles, which can pass the nasal airways and penetrate down to the lung [24]. Since a case report describing lung injury by "white dust" [15] suggested that the particles from ultrasonic humidifiers may exert adverse effects on the lung, we examined the effects in detail using a mouse model. Although the bacterial contamination was not investigated in the present study, chlorine-disinfected tap water, a commercial mineral water for drinking, and purified water were used for the experiments to minimize the contamination. In general, the insoluble component of the particles are not dissolved and deposit in pulmonary surfactant, where they are taken up by alveolar macrophages [25,26]. The inhaled particles taken up by the macrophages are transferred to intracellular vesicle and phagolysosome [27], exposed to acidic milieu, and can cause lysosome destabilization leading to inflammation [28]. TEM observation in the present study showed that the particles were being dissolved in the phagosome, and also indicated that the particles generated by the ultrasonic humidifier disintegrated in the phagolysosome of the macrophages. This observation was consistent with our microarray data suggesting that genes dysregulated by the particles from the ultrasonic humidifier were enriched in GO categories associated with MHC molecules and endocytosis. However, expression of *H2-Eb1* was suppressed by inhalation of particles from the humidifier with tap water or high-

silica water. The result was in opposition to the effect of pulmonary exposure (intratracheal instillation) to titanium dioxide nanoparticles [29] and fullerenes [30] on the lung, suggesting that 7- and 14-day inhalation of the particles from the humidifier induced a cellular response from the alveolar macrophages but did not cause acute or sub-acute toxic effects on the lung tissue. This observation was supported by RT-PCR data suggesting that no significant difference in *Ccl2*, *Cxcl1*, and *Tnf* expression between the tap water or high-silica water group and each control (ultrapure water) group. A previous study showed that inhalation of silica-coated nanoparticles (10 mg/m^3; 2 hr/day for 4 days) enhanced *Cxcl1* and *Tnf* expression in mouse lung [23]. Even though the total exposure period in the present study was longer than this previous study, the concentration of airborne particles containing silica from the humidifier was lower. The genes differentially expressed by inhalation of particles from the humidifier were enriched in mitosis, meiosis and related GO and pathways. However, histopathology (including cell proliferation) and macrophage location were not affected by the particles derived from tap water or high-silica water. Our data on the mononuclear cells in BALF indicated that alveolar macrophages tended to be activated by the aerosol particles. The results suggested that 7- and 14-day inhalation of the particles from the humidifier did not cause acute or sub-acute toxic effects on the lung of mice without pre-existing respiratory infection, disease or malfunction.

Conclusion

The present study showed the characteristics of particles generated from ultrasonic humidifiers operated with tap water, a commercial mineral (high-silica) water, and other types of water. This study also showed the effect of 7- and 14-day inhalation of particles released from the humidifier on the lung in a mouse model. The particles were composed of multiple elements including sodium, magnesium, silicate, sulfate, and calcium. Mass and number concentrations and the peak size of the particles were positively correlated to concentration of dissolved mineral components in water provided to the humidifier. Inhalation of particles caused dysregulation of genes related to mitosis, cell adhesion molecules, MHC molecules and endocytosis followed by antigen processing, but did not induce any signs of inflammation or tissue injury in the lung. We conclude that the particles released from the humidifier operated with tap water and commercial mineral water induced a cellular response from the alveolar macrophages but did not cause acute or sub-acute toxic effects on the pulmonary organs in the mouse model. Finally, since the mass concentration of particles generated is linearly correlated with the concentration of dissolved material in water, cautions may be needed to use the humidifier in some areas with hard water. Long exposure to the aerosol particle from the humidifier may occur in home and working environment. High mineral content tap water is not recommended and de-mineralized water should be recommended in order to exclude any adverse effects.

Additional file

Additional file 1: Table S1. *Primer and probe sequences for quantitative RT-PCR.* **Figure S1.** Profile of gene expression in the lung exposed to aerosol released from ultrasonic humidifier with tap water, high-silica water, or ultrapure water. **Table S2.** Differentially expressed genes with relevant enriched GO and pathways.

Abbreviations

BALF: Bronchoalveolar lavage fluid; cDNA: Complementary DNA; EDS: Energy-dispersive X-ray spectrometer; FE-SEM: Field emission-type scanning electron microscope; GO: Gene ontology; ICP-MS: Inductively coupled plasma mass spectrometry; RO: Reverse osmotic; TDS: Total dissolved solids; TEM: Transmission electron microscope.

Competing interests

The authors declare that they have no competing interests.

Authors' contributions

KT is the main project leader. KT and MU conceived the overall research idea. KSe mainly performed all experiment procedures and data analyses. MU, KSu, MK-I, TI and MS were substantially involved in conducting the experiments and data analyses. MU mainly conducted microarray data analysis. KSu, a specialist in combining nanotechnology and biology, analyzed airborne particles by electron microscopy with KSe. MK-I, an expert on electron microscopy, analyzed particles in the tissue sections with KSe and MU. TI and MS conducted data analyses with pathological and clinical viewpoints. MU and KSe drafted the manuscript. All authors read and approved the final manuscript.

Acknowledgements

We thank the graduate and undergraduate students in the Takeda laboratory, especially Mr. Ryuhei Shimizu and Mr. Hiroshi Hori, for their technical assistance. This work was supported in part by a MEXT-Supported Program for the Strategic Research Foundation at Private Universities (Ken Takeda; 2011–2015) and a JSPS KAKENHI Grant Number 24790130 (Masakazu Umezawa; 2012–2013).

Author details

[1]Department of Hygienic Chemistry, Faculty of Pharmaceutical Sciences, Tokyo University of Science, 2641 Yamazaki, Noda, Chiba 278-8510, Japan. [2]The Center for Environmental Health Science for the Next Generation, Research Institute for Science and Technology, Tokyo University of Science, 2641 Yamazaki, Noda, Chiba 278-8510, Japan. [3]Department of Pathology, Tochigi Institute of Clinical Pathology, 2308-3 Sasayama, Minami-akatsuka, Nogi-machi, Shimotsuga-gun, Tochigi 329-0112, Japan.

Received: 28 August 2013 Accepted: 17 December 2013
Published: 21 December 2013

References

1. Klepeis NE, Nelson WC, Ott WR, Robinson JP, Tsang AM, Switzer P, Behar JV, Hern SC, Engelmann WH: **The National Human Activity Pattern Survey (NHAPS): a resource for assessing exposure to environmental pollutants.** *J Expo Anal Environ Epidemiol* 2001, 11:231–252.
2. Norbäck D, Torgén M, Edling C: **Volatile organic compounds, respirable dust, and personal factors related to prevalence and incidence of sick building syndrome in primary schools.** *Br J Ind Med* 1990, 47:733–741.
3. Harrison J, Pickering CA, Faragher EB, Austwick PK, Little SA, Lawton L: **An investigation of the relationship between microbial and particulate indoor air pollution and the sick building syndrome.** *Respir Med* 1992, 86:225–235.

4. Carrer P, Maroni M, Alcini D, Cavallo D: **Allergens in indoor air: environmental assessment and health effects.** *Sci Total Environ* 2001, **270**:33–42.
5. Oeder S, Dietrich S, Weichenmeier I, Schober W, Pusch G, Jörres RA, Schierl R, Nowak D, Fromme H, Behrendt H, Buters JT: **Toxicity and elemental composition of particulate matter from outdoor and indoor air of elementary schools in Munich, Germany.** *Indoor Air* 2012, **22**:148–158.
6. Fang L, Wyon DP, Clausen G, Fanger PO: **Impact of indoor air temperature and humidity in an office on perceived air quality, SBS symptoms and performance.** *Indoor Air* 2004, **14**(Suppl):74–81.
7. Melikov AK, Skwarczynski MA, Kaczmarczyk J, Zabecky J: **Use of personalized ventilation for improving health, comfort, and performance at high room temperature and humidity.** *Indoor Air* 2013, **23**:250–263.
8. Environmental protection Agency: *Indoor Air Facts No.8 Use and Care of Home Humidifiers.* 1991. http://www.epa.gov/iaq/pdfs/humidifier_factsheet.pdf.
9. Kane GC, Marx JJ, Prince DS: **Hypersensitivity pneumonitis secondary to *Klebsiella oxytoca*, A new cause of humidifier lung.** *Chest* 1993, **104**:627–629.
10. Suda T, Sato A, Ida M, Gemma H, Hayakawa H, Chida K: **Hypersensitivity pneumonitis associated with home ultrasonic humidifiers.** *Chest* 1995, **107**:711–717.
11. Tyndall LR, Lehman SE, Bowman KE, Milton KD, Barbaree MJ: **Home humidifiers as a potential source of exposure to microbial pathogens endotoxins and allergens.** *Indoor Air* 2004, **5**:171–178.
12. Cheong HK, Ha M, Lee JH: **Unrecognized bomb hidden in the babies' room: fetal pulmonary damage related with use of biocide in humidifiers.** *Environ Health Toxicol* 2012, **162**:e2012001.
13. Rodes C, Smith T, Crouse R, Ramachandran G: **Measurements of the size distribution of aerosols produced by ultrasonic humidification.** *Aerosol Sci Technol* 1990, **13**:220–229.
14. Highsmith VR, Rodes CE, Hardy RJ: **Indoor particle concentrations associated with use of tap water in portable humidifiers.** *Environ Sci Technol* 1988, **22**:1109–1112.
15. Daftary AS, Deterding RR: **Inhalational lung injury associated with humidifier "white dust".** *Pediatrics* 2011, **127**:e509–e512.
16. Brazma A, Hingamp P, Quackenbush J, Sherlock G, Spellman P, Stoeckert C, Aach J, Ansorge W, Ball CA, Causton HC, Gaasterland T, Glenisson P, Holstege FC, Kim IF, Markowitz V, Matese JC, Parkinson H, Robinson A, Sarkans U, Schulze-Kremer S, Stewart J, Taylor R, Vilo J, Vingron M: **Minimum information about a microarray experiment (MIAME)-toward standards for microarray data.** *Nat Genet* 2001, **29**:365–371.
17. Quackenbush J: **Computational analysis of microarray data.** *Nat Rev Genet* 2001, **2**:418–427.
18. Eisen MB, Spellman PT, Brown PO, Botstein D: **Cluster analysis and display of genome-wide expression patterns.** *Proc Natl Acad Sci USA* 1998, **95**:14863–14868.
19. Saldanha AJ: **Java treeview–extensible visualization of microarray data.** *Bioinformatics* 2004, **20**:3246–3248.
20. **DATA folder in FTP site of National Center for Biotechnology Information.** ftp://ftp.ncbi.nih.gov/gene/DATA/.
21. **MSigDB/Download in the GSEA site of Broad Institute.** http://www.broadinstitute.org/gsea/downloads.jsp#msigdb.
22. Hung DV, Tong S, Nakano Y, Tanaka F, Hamanaka D, Uchino T: **Measurements of particle size distributions produced by humidifiers operating in high humidity storage environments.** *Biosyst Eng* 2010, **107**:54–60.
23. Rossi EM, Pylkkänen L, Koivisto AJ, Vippola M, Jensen KA, Miettinen M, Sirola K, Nykäsenoja H, Karisola P, Stjernvall T, Vanhala E, Kiilunen M, Pasanen P, Mäkinen M, Hämeri K, Joutsensaari J, Tuomi T, Jokiniemi J, Wolff H, Savolainen K, Matikainen S, Alenius H: **Airway exposure to silica-coated TiO_2 nanoparticles induces pulmonary neutrophilia in mice.** *Toxicol Sci* 2010, **113**:422–433.
24. Oberdörster G, Oberdörster E, Oberdörster J: **Nanotoxicology: an emerging discipline evolving from studies of ultrafine particles.** *Environ Health Perspect* 2005, **113**:823–839.
25. Geiser M, Kreyling WG: **Deposition and biokinetics of inhaled nanoparticles.** *Part Fibre Toxicol* 2010, **7**:2.
26. Scherbart AM, Langer J, Bushmelev A, Van Berlo D, Haberzettl P, Van Schooten FJ, Schmidt AM, Rose CR, Schins RP, Albrecht C: **Contrasting macrophage activation by fine and ultrafine titanium dioxide particles is associated with different uptake mechanisms.** *Part Fibre Toxicol* 2011, **8**:31.
27. Geiser M, Casaulta M, Kupferschmid B, Schulz H, Semmler-Behnke M, Kreyling W: **The role of macrophages in the clearance of inhaled ultrafine titanium dioxide particles.** *Am J Respir Cell Mol Biol* 2008, **38**:371–376.
28. Donaldson K, Schinwald A, Murphy F, Cho WS, Duffin R, Tran L: **The biologically effective dose in inhalation nanotoxicology.** *Acc Chem Res* 2013, **46**:723–732.
29. Park EJ, Yoon J, Choi K, Yi J, Park K: **Induction of chronic inflammation in mice treated with titanium dioxide nanoparticles by intratracheal instillation.** *Toxicology* 2009, **260**:37–46.
30. Park EJ, Kim H, Kim Y, Yi J, Choi K, Park K: **Carbon fullerenes (C_{60}s) can induce inflammatory responses in the lung of mice.** *Toxicol Appl Pharmacol* 2010, **244**:226–233.

doi:10.1186/1743-8977-10-64
Cite this article as: Umezawa *et al.*: Effect of aerosol particles generated by ultrasonic humidifiers on the lung in mouse. *Particle and Fibre Toxicology* 2013 **10**:64.

PLOS ONE

Gene Expression Changes in the Olfactory Bulb of Mice Induced by Exposure to Diesel Exhaust Are Dependent on Animal Rearing Environment

Satoshi Yokota[1,2]*, Hiroshi Hori[1], Masakazu Umezawa[2], Natsuko Kubota[2], Rikio Niki[2], Shinya Yanagita[2,3], Ken Takeda[1,2]

1 Department of Hygiene Chemistry, Faculty of Pharmaceutical Sciences, Tokyo University of Science, 2641 Yamazaki, Noda, Chiba, Japan, **2** The Center for Environmental Health Science for the Next Generation, Research Institute for Science and Technology, Tokyo University of Science, 2641 Yamazaki, Noda, Chiba, Japan, **3** Faculty of Science and Technology, Tokyo University of Science, 2641 Yamazaki, Noda, Chiba, Japan

Abstract

There is an emerging concern that particulate air pollution increases the risk of cranial nerve disease onset. Small nanoparticles, mainly derived from diesel exhaust particles reach the olfactory bulb by their nasal depositions. It has been reported that diesel exhaust inhalation causes inflammation of the olfactory bulb and other brain regions. However, these toxicological studies have not evaluated animal rearing environment. We hypothesized that rearing environment can change mice phenotypes and thus might alter toxicological study results. In this study, we exposed mice to diesel exhaust inhalation at 90 $\mu g/m^3$, 8 hours/day, for 28 consecutive days after rearing in a standard cage or environmental enrichment conditions. Microarray analysis found that expression levels of 112 genes were changed by diesel exhaust inhalation. Functional analysis using Gene Ontology revealed that the dysregulated genes were involved in inflammation and immune response. This result was supported by pathway analysis. Quantitative RT-PCR analysis confirmed 10 genes. Interestingly, background gene expression of the olfactory bulb of mice reared in a standard cage environment was changed by diesel exhaust inhalation, whereas there was no significant effect of diesel exhaust exposure on gene expression levels of mice reared with environmental enrichment. The results indicate for the first time that the effect of diesel exhaust exposure on gene expression of the olfactory bulb was influenced by rearing environment. Rearing environment, such as environmental enrichment, may be an important contributive factor to causation in evaluating still undefined toxic environmental substances such as diesel exhaust.

Citation: Yokota S, Hori H, Umezawa M, Kubota N, Niki R, et al. (2013) Gene Expression Changes in the Olfactory Bulb of Mice Induced by Exposure to Diesel Exhaust Are Dependent on Animal Rearing Environment. PLoS ONE 8(8): e70145. doi:10.1371/journal.pone.0070145

Editor: Brian Key, School of Biomedical Sciences, The University of Queensland, Australia

Received March 10, 2013; **Accepted** June 16, 2013; **Published** August 5, 2013

Funding: This work was supported by Grant-in-Aid for JSPS Fellows (Satoshi Yokota, 22. 5895) and in part by a Grant-in-Aid for Science Research from the Ministry of Education, Culture, Sports, Science and Technology of Japan. This work was also supported by a Grant-in Aid for the Private University Science Research Upgrade Promotion Business "Academic Frontier Project, a Grant-in Aid for Health and Labour Sciences Research Grants, Research on Risk of Chemical Substances, from the Ministry of Health, Labour and Welfare" and a Grant-in Aid for NEXT-Supported Program for the Strategic Research Foundation at Private Universities, 2011–2015. The funders had no role in study design, data collection and analysis, decision to publish, or preparation of the manuscript.

Competing Interests: The authors have declared that no competing interests exist.

* E-mail: satoshi_yokota1008@yahoo.co.jp

Introduction

Diesel exhaust (DE) consists of a complex mixture of components in gaseous or particulate form (DEP: diesel exhaust particles). DEP comprise more than 1,000 chemicals that are mainly composed of cores of elemental carbon, traces of metallic compounds, and adsorbed organic materials including polycyclic aromatic hydrocarbons, aldehydes, and nitrogen oxides [1]. DEP accumulate and negatively affect lung function following inhalation exposure. It has been reported that DE causes lung cancer [2], allergic rhinitis [3], and bronchial asthma-like diseases [4]. In fact, the International Agency for Research on Cancer, which is part of the World Health Organization, classified DE as carcinogenic to humans (Group 1) in 2012, based on sufficient evidence that DE exposure is associated with an increased risk of lung cancer [5].

Some research has led to the concern that the brain represents a target for the effects of ambient particulate matter (PM), mainly derived from DEP in urban environments [6]. It has been demonstrated that a small fraction of inhaled nanoparticles may reach the brain [7,8]. Nanoparticles deposit in alveolar and subsequently cross the lung–blood barrier and the blood–brain barrier, and small nanoparticles, especially those below 10 nm, deposit efficiently on the olfactory mucosa by diffusion. Subsequent uptake and translocation of nanoparticles along axons of olfactory nerves has been reported [9,10]. Previous *in vitro* studies have demonstrated that nanoparticles, such as DEP, might cause neurotoxic effects and disturb blood–brain barrier function [11,12]. In addition, *in vivo* studies also have demonstrated that DE inhalation exposure has inflammatory effects on the olfactory bulb and midbrain regions of the brain [13,14].

However, these toxicological studies have not evaluated the effects of conditions in the animal rearing environment. Effects of exposure to environmental chemicals and materials including nanoparticles are usually assessed in a standard laboratory cage environment alone. Mice housed in standard laboratory cages demonstrate frequent stereotyped behavior, in particular sponta-

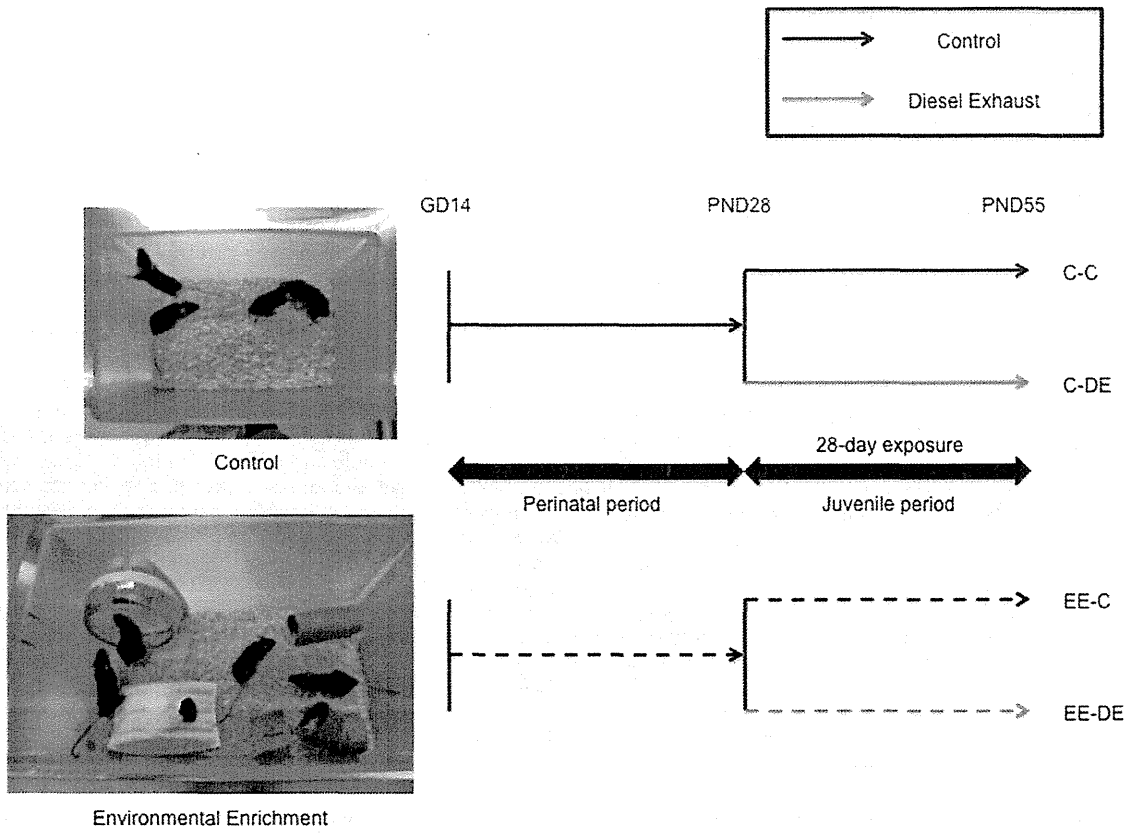

Figure 1. Schematic diagram of design of the present study.
doi:10.1371/journal.pone.0070145.g001

neous jumping and backward flipping, which is persistent and occurs early in development compared with those housed in environmental enrichment conditions [15]. In contrast, environmental enrichment, which provides a combination of complex inanimate and social stimulation, may improve the well-being of animals reared in standard housing [16]. It has been reported that environmental enrichment attenuated stereotyped behavior compared with a standard laboratory housing environment [17]. Stereotyped behavior is a feature of autism [18] and is often observed in persons with mental retardation or developmental disorders [19,20,21]. Standard housing environment may change mice phenotypes [22] and thus might alter toxicological research results.

We hypothesized that chemical substance exposure-induced toxicity might be influenced by housing environment. In fact, it has been recommended that rodents reared in environmental enrichment should be used for regulatory toxicological research [23]. In particular, the rearing environment during the perinatal period is important for the development of the central nervous system of offspring [24], which suggests the possibility that early rearing environment might change the susceptibility of animals to chemical substance exposure. However, there are no data that have investigated if early rearing environment alters the later effects of DE exposure on the central nervous system.

We focused on the olfactory bulb because the olfactory translocation route is one of the targets of DEP [25]. The objective of the present study was to gain insight into how gene expression changes in the olfactory bulb of mice reared in a standard cage environment compare with those reared in environmental enrichment during the perinatal period when they were exposed to DE.

Materials and Methods

Animals

Pregnant C57BL/6J mice, weighing approximately 30 g (Figure S1A) at gestational day 14, were purchased from CLEA Japan, Inc. (Tokyo, Japan) and used for experiments. All animals were acclimated to our animal room (The Center for Environmental Health Science for the Next Generation, Research Institute for Science and Technology, Tokyo University of Science). They had free access to water and standard animal food and were exposed to a 12-hour light/dark cycle (lights on between 8:00 and 20:00), a temperature of 22±1°C, and a humidity-controlled environment (50±5%). Body weights of dams and their pups were recorded at sampling (Figure S1B–D). All experiments were performed in accordance with Animal Research: Reporting In Vivo Experiments guidelines for the care and use of laboratory animals [26] and were approved by Tokyo University of Science's Institutional Animal Care and Use Committee. All sampling was performed under sodium pentobarbital (50 mg/kg) anesthesia, and all efforts were made to minimize suffering.

Housing Environmental Conditions

Upon arrival to the colony, half of the 20 pregnant dams were assigned to the standard cage environment (C) and the other half

Table 1. Design of primer pairs for Real-Time RT-PCR analysis.

Gene symbol		Sequence (5'>3')	Tm (°C)	GenBank Accession
Gapdh	Forward:	TGTGCAGTGCCAGCCTCGTC	60	NM_008084
	Reverse:	GGATGCATTGCTGACAATCT		
Dbp	Forward:	AAGCATTCCAGGCCATGAGAC	60	NM_016974
	Reverse:	CGGCTCCAGTACTTCTCATC		
Cxcl10	Forward:	CCGGAAGCCTCCCCATCAGC	60	NM_021274
	Reverse:	GGGATCCCTTGAGTCCCACTCAGAC		
Chmp4b	Forward:	GATGGCACCCTGTCAACCATC	60	NM_029362
	Reverse:	TGAGCTCATCCTCGTCGAAC		
Fam13c	Forward:	AGCTGAAGCTGTCGGAAGAGC	60	NM_024244
	Reverse:	GATACCTCTGCATCGGTCATA		
Mslnl	Forward:	GGCTTACTGTCATGCAGACTG	60	NM_177822
	Reverse:	AAGTGGCCTTGGACTCTAGG		
Umodl1	Forward:	AACTATAGCGTGTCCGCCAG	60	NM_177465
	Reverse:	TGCAGTGCAGGTAGACGATG		
Aqp3	Forward:	ATCTATGCACTGGCACAGAC	60	NM_016689
	Reverse:	ATTGACCATGTCCAAGTGTC		
Cyp2f2	Forward:	GAAGTCGCTTCGACTATGAC	60	NM_007817
	Reverse:	TCCATATTGAAGTGGCTCAG		
Krt18	Forward:	AGATTGCCAGCTCTGGATTG	60	NM_010664
	Reverse:	TGGTGACAACTGTGGTACTC		
Sdad1	Forward:	TGCTGCAGAACTTCATGTAC	60	NM_172713
	Reverse:	CACGCAGTTGTGATAACATTG		
Nr1i3	Forward:	TGCTACAAGATGGAGGACGC	60	NM_009803
	Reverse:	TTGTTCAGAATCAGCGCCATC		

Table 1 shows the gene symbol, primer pair sequences, T_m, and GenBank accession numbers for the corresponding genes.
Footnote: T_m is the melting temperature of the PCR product.
doi:10.1371/journal.pone.0070145.t001

to environmental enrichment (EE). Standard laboratory cage consisted of a common housing cage for mice (30×20×12.5 cm: 7500 cm^3). Environmental enrichment consisted of a larger (40×25×19 cm: 19,000 cm^3) cage containing a running wheel, small house, wood blocks, and plastic tubing that were moved to different locations within each cage every 2–3 days and were exchanged with new toys. One dam and her pups (n = 8) were housed in either the standard laboratory cage or environmental enrichment throughout the perinatal period and until weaning. After weaning at postnatal day 27, the offspring mice were placed

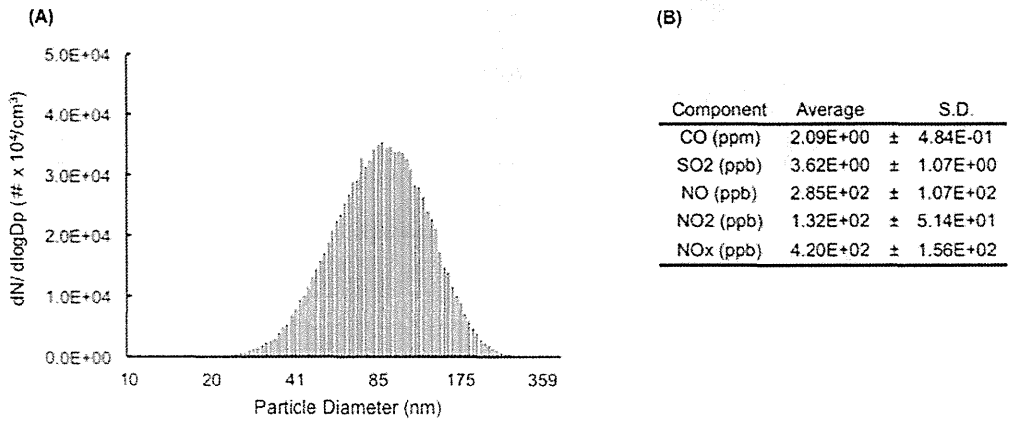

Figure 2. Characterization of diesel exhaust. (A) Particle diameter distribution of diesel exhaust particles. (B) Concentrations of gaseous components.
doi:10.1371/journal.pone.0070145.g002

in a control chamber or DE inhalation chamber and were housed under the same conditions as during the perinatal period. The mice were exposed to DE for 8 hours/day (10:00–18:00) for 28 days (postnatal days 28−55) in the control or DE inhalation chamber at the Center for Environmental Health Science for the Next Generation (Research Institute for Science and Technology, Tokyo University of Science). Housing environment (standard cage environment [C] or environmental enrichment [EE]) during the perinatal period (gestational day 14–postnatal day 28) and chamber (control [C] and [DE]) established four experimental groups: C-C, C-DE, EE-C, and EE-DE (Figure 1). Necropsies were performed 1 day after the final exposure. In this experiment, 7–9 independent litters (C-C: n = 7, C-DE: n = 7, EE-C: n = 8, EE-DE: n = 9) were used. The olfactory bulb was collected from each male mouse, frozen quickly in liquid nitrogen, and then stored at −80°C until total RNA extraction. Lung tissues were also collected and immersed in 10% phosphate buffered formalin until use.

Diesel Exhaust

A four-cylinder 2,179 cc diesel engine (Isuzu Motors Ltd., Tokyo, Japan) was operated at a speed of 1500 rpm and 80% load with diesel fuel. The exhaust was introduced into a stainless steel dilution tunnel (216.3 mm diameter × 5250 mm) where the exhaust was mixed with clean air. Particle size distributions (measuring range 10–410 nm) were investigated using a scanning mobility particle sizer apparatus (model 3936, TSI Inc., St. Paul, MN, USA) composed of a condensation particle counter (model 3785, TSI Inc.) and a differential mobility analyzer (model 3081, TSI Inc.). The apparatus was operated at a sample flow rate of 0.6 L/minute and a sheath flow rate of 6.0 L/minute. The mass and number concentrations of DEP were measured by a Piezobalance Dust Monitor (model 3521, Kanomax, Inc., Osaka, Japan) and a condensation particle counter (model 3007, TSI Inc.), respectively. Concentrations of gas components, [i.e., nitric oxide (NO_x), sulfur dioxide (SO_2), and carbon monoxide (CO)] in the chambers were measured by an NO-NO_2-NO_x analyzer model 42i (Thermo Fisher Scientific Inc., Franklin, MA, USA), Enhanced Trace Level SO_2 Analyzer, Model 43i-TLE (Thermo Fisher Scientific Inc.), and a CO Analyzer, model 48i (Thermo Fisher Scientific Inc.), respectively.

Immunohistochemistry

Dams at the weaning period were perfused transcardially with a heparin solution (1000 U/l, 0.9% saline), followed by ice-cooled fixative composed of 4% paraformaldehyde, 0.1% glutaraldehyde, and 0.2% picric acid in 0.1 M phosphate buffered saline (PBS, pH 7.4). The brains were removed and post-fixed in the same

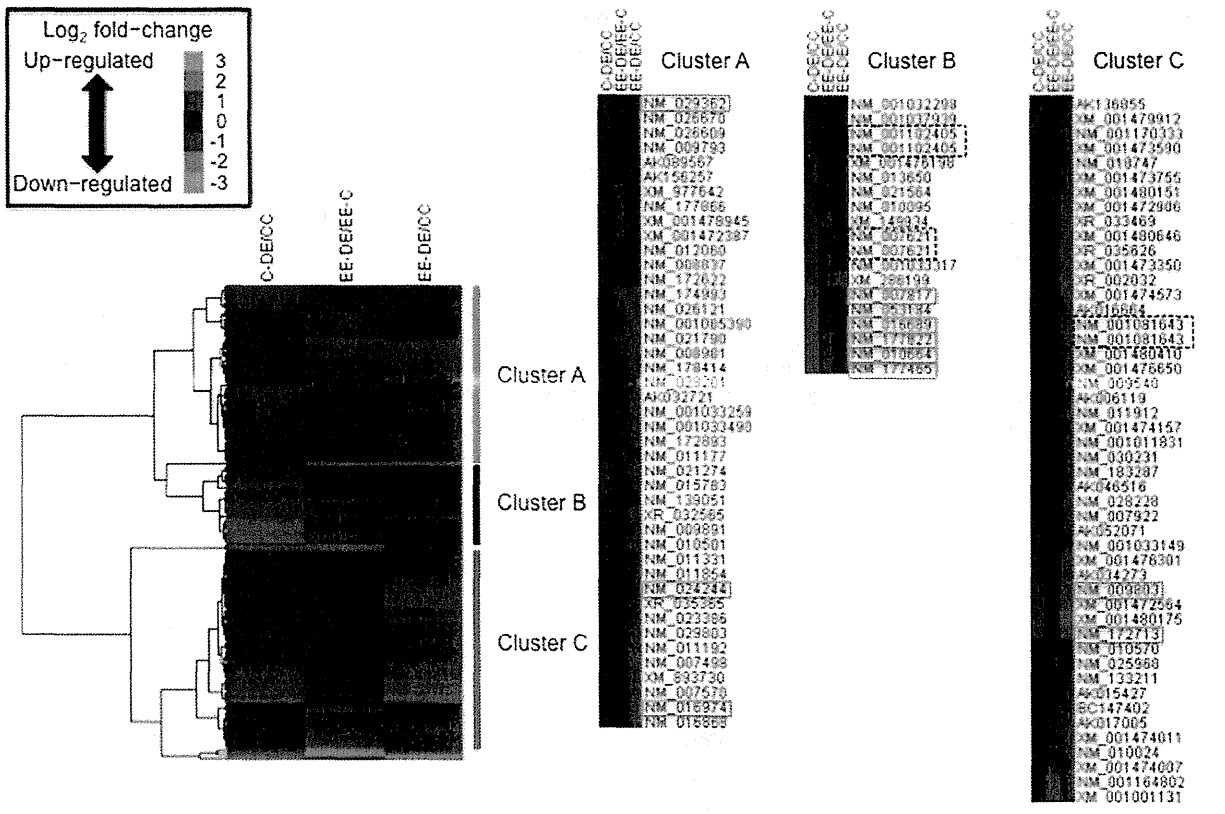

Figure 3. Hierarchical clustering of gene expression data. Within each group, a fold change (C-DE/C-C, EE-DE/EE-C, and EE-DE/C-C) was calculated and $\log_2$ transformed for all 116 spots on the microarray that did not have any missing values. These values were then hierarchically clustered using Euclidean distance metric and complete linkage. The colored images are presented as described: the color scale ranges from saturated green for $\log_2$ ratios −3.0 and below to saturated red for $\log_2$ ratios 3.0 and above. Gene expression profiles were divided into 3 clusters (clusters A, B, and C), and quantitative RT-PCR analysis was performed for genes surrounded by the red line in each cluster. Genes surrounded by black dotted line were the same gene derived from different spots.
doi:10.1371/journal.pone.0070145.g003

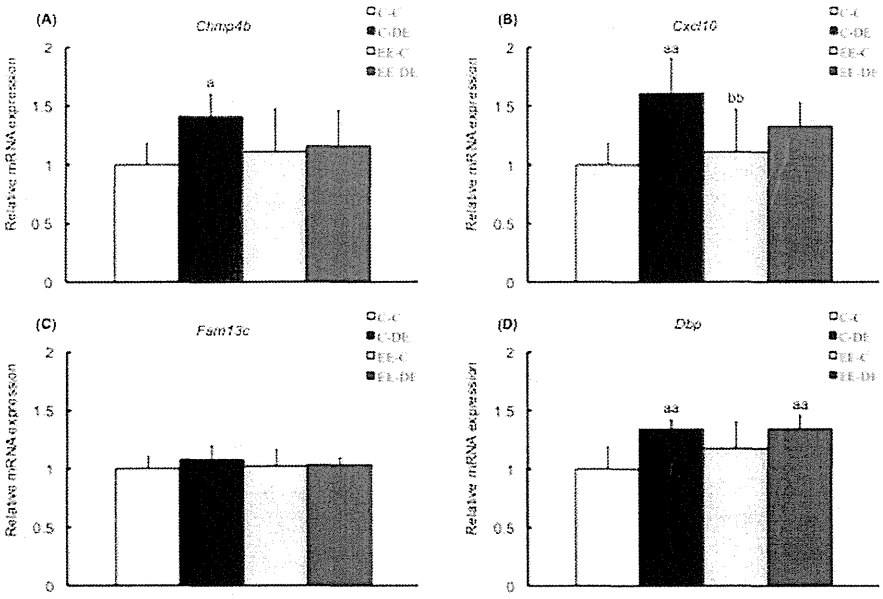

Figure 4. Confirmation of microarray data in cluster A by RT-PCR. Data show mRNA expressions for (A) *Chmp4b*, (B) *Cxcl10*, (C) *Fam13c*, and (D) *Dbp* in the olfactory bulb of mice in each group. *Chmp4b*, *Cxcl10*, and *Dbp*, except for *Fam13c*, of mice reared in a standard cage environment were significantly upregulated by exposure to diesel exhaust. There was no significant effect of exposure to diesel exhaust on gene expressions of mice reared in environmental enrichment. The data are expressed as relative target gene expression compared with *Gapdh* expression. Each column represents the mean ± standard deviation (C-C: n = 7, C-DE: n = 7, EE-C: n = 8, EE-DE: n = 9). Data were analyzed by two-way analysis of variance as described in the Methods section. An analysis of simple effects is as follows: *Chmp4b*: a indicates significant differences (Tukey–Kramer method, $^{a}P<0.05$, C-C vs. C-DE); *Cxcl10*: a indicates significant differences (Tukey–Kramer method, $^{aa}P<0.01$, C-C vs. C-DE); b indicates significant differences (Tukey–Kramer method, $^{bb}P<0.01$, C-DE vs. EE-C); and *Dbp*: a indicates significant differences (Tukey–Kramer method, $^{aa}P<0.01$, C-C vs. C-DE and C-C vs. EE-DE).
doi:10.1371/journal.pone.0070145.g004

fixative without glutaraldehyde for 24 hours at 4°C. The brains were then cryoprotected in a phosphate-buffered 30% sucrose solution with 0.1% sodium azide for 24–48 hours. The brains were then frozen and cut in the coronal plane (6 series of 40- μm thick sections) on a microtome (Sakura Finetek Co., Ltd., Japan) and collected in 0.1 M PBS with 0.1% sodium azide.

Immunohistochemical visualization of FosB was performed on free-floating sections using antibody and avidin-biotin peroxidase methods as previously described [27,28]. Briefly, after blocking endogenous peroxidase and preincubation in 10% normal horse serum, the sections were incubated in primary rabbit polyclonal affinity purified anti-FosB antibody (sc-48, Santa Cruz Biotechnology, Inc., Santa Cruz, CA, USA) diluted 1:600 in 0.1 M PBS with 0.1% Triton X-100 for 16 hours at room temperature. After three 10-minute rinses in 0.1 M PBS with 0.1% Triton X-100, the sections were further incubated in a biotinylated secondary antibody solution, donkey anti-rabbit IgG (AP182B, Chemicon, Temecula, CA, USA, 1:800) for 120 minutes at room temperature, followed by three 10-minute rinses in 0.1 M PBS with 0.1% Triton X-100, and finally treated with an avidin-biotin peroxidase complex (Vectastain ABC peroxidase kit, Vector Laboratories Inc., Burlingame, CA, USA, 1:400) for 240 minutes. The sections were reacted for peroxidase activity in a solution consisting of nickel ammonium sulfate, 0.02% 3,3-diaminobenzidine in 0.1 M Tris-HCl buffer (pH 7.6), and 0.01% H_2O_2 for 20 minutes. FosB immunoreactivity was localized to the cell nuclei and appeared as a dark gray-black stain. Subsequently, sections were washed in 0.01 M PBS, mounted on gelatin-coated glass slides, air-dried, dehydrated in a graded series of alcohols, cleared in xylene, and coverslipped with Entellan (Merck Co, Ltd., Japan). Photomicrographs were captured with a light microscope (BX51; Olympus Co., Ltd., Japan).

Hematoxylin-eosin Staining

Lung tissues were embedded in paraffin, cut on the microtome, and then stretched in a water bath. Paraffin-embedded lung sections were removed from the water bath and air-dried for 1 hour at 40°C on slides. Staining was performed manually in staining dishes as follows: a de-washing step in xylene, then rehydration with successive incubations in 95% ethanol, and finally tap water. Hematoxylin 3G (Sakura Finetek Co., Ltd., Japan) was applied for 5 minutes followed by a wash with running tap water for 5 minutes and staining with eosin (Sakura Finetek Co., Ltd., Japan) for 3 minutes. After washing with tap water and dehydration with successive washes of 95% ethanol and xylene, slides were mounted by Entellan and air-dried prior to microscopic examination.

Total RNA Isolation

Olfactory bulbs were immediately isolated (within 50 seconds), frozen in liquid nitrogen, and kept at −80°C. Total RNA was isolated using Isogen (Nippon Gene Co., Ltd., Tokyo, Japan) according to the manufacturer's protocol and suspended in pure water. The RNA quantity was determined by spectrophotometry measurement of OD260/280 (ratio >1.8) in a BioPhotometer plus (Eppendorf, Hamburg, Germany). Extracted RNA from each sample was used for microarray and quantitative RT-PCR analysis.

Table 2. Functional analysis of microarray data using Gene Ontology (GO).

GO ID	Term	Nf	P value	Enrichment factor	GenBank Accession	Gene symbol
GO:0051607	defense response to virus	62	<0.001	11.41	NM_021274	Cxcl10
					NM_010501	Ifit3
					NM_011854	Oasl2
					NM_133211	Tlr7
					NM_015783	Isg15
GO:0006954	inflammatory response	94	<0.001	7.52	NM_009793	Camk4
					NM_021274	Cxcl10
					NM_013650	S100a8
					NM_011331	Ccl12
					NM_133211	Tlr7
GO:0045087	innate immune response	97	<0.001	7.29	NM_010501	Ifit3
					NM_013650	S100a8
					NM_011854	Oasl2
					NM_001170333	Clec4a2
					NM_133211	Tlr7
GO:0006955	immune response	62	<0.001	9.13	NM_021274	Cxcl10
					NM_011331	Ccl12
					NM_011854	Oasl2
					NM_012060	Bcap31
GO:0006935	chemotaxis	41	<0.01	10.35	NM_021274	Cxcl10
					NM_013650	S100a8
					NM_011331	Ccl12
GO:0009615	response to virus	32	<0.01	13.26	NM_010501	Ifit3
					NM_011854	Oasl2
					NM_029803	Ifi27l2a
GO:0007608	sensory perception of smell	31	<0.01	13.69	NM_053184	Ugt2a1
					NM_001033317	Cnga4
					NM_001011831	Olfr1500
GO:0008009	chemokine activity	14	<0.01	20.21	NM_021274	Cxcl10
					NM_011331	Ccl12

doi:10.1371/journal.pone.0070145.t002

Complementary DNA Microarray Procedures

After purification of RNA by ethanol precipitation and an RNeasy Micro Kit (Qiagen, Hilden, Germany), the RNA integrity was evaluated by capillary electrophoresis using a Bioanalyzer 2100 (Agilent Technologies, Inc., Santa Clara, CA, USA). Each RNA sample (31 individual samples) showed 8.8−9.9 in the RNA integrity number scores. To reduce false positives due to variability between individual samples, equal amounts of total RNAs from individual samples from each cage (one olfactory bulb sample/cage) were pooled (7−9 sample pooling in each group). To improve the accuracy of the data, the pooled RNA template was divided into two replicates for technical analysis. In this pooled data set, the average data between two replicate arrays were used for microarray analysis. Each of the pooled RNA samples was labeled with Cy3 and hybridized to a SurePrint G3 Mouse GE 8×60K microarray (Agilent Technologies) consisting of 62,976 spots (28,620 genes) according to the protocol of DNA Chip Research Inc. (Kanagawa, Japan). After hybridization with fluorescent-labeled cDNA, the microarray was washed using Gene Expression Wash Buffers Pack (Agilent Technologies) and then scanned by a DNA microarray Scanner G2565CA (Agilent Technologies). Scanner output images were normalized and digitalized by Agilent Feature Extraction software according to the Minimum Information about a Microarray Experiment guidelines [29] and a pre-processing method for Agilent data [30]. The raw data and normalized data have been deposited in NCBI's Gene Expression Omnibus and are accessible thorough Gene Expression Omnibus Series accession number GSE46163 (http://www.ncbi.nlm.nih.gov/geo/query/acc.cgi?acc = GSE46163).

Hierarchical Cluster Analysis

To extract characteristic gene sets that were differentially expressed after subacute exposure to DE, the $\log_2$ fold-change data (C-C vs. C-DE, EE-C vs. EE-DE, and C-C vs. EE-DE comparison in offspring) of gene expression were hierarchically clustered using a complete linkage algorithm and Euclidean distance as the

distance metric [31]. The analysis was performed using Cluster 3.0 [32], and the result was visualized by Java TreeView [33].

Defining Functional Relationships between Expression Profiles

To better understand the biological meanings of the microarray results, functional analyses were performed using gene annotation by Gene Ontology (GO) and canonical pathway analysis. All genes printed on the microarray were annotated with GO using an annotation file (ftp://ftp.ncbi.nih.gov/gene/DATA/gene2go.gz) provided by National Center for Biotechnology Information (NCBI; Bethesda, MD) and pathway analysis using c2.cp.v3.1.symbols.gmt in http://www.broadinstitute.org/gsea/downloads.jsp#msigdb provided by Broad Institute (BI; Cambridge, MA). The annotation was updated in January 2013. All of the differentially expressed genes were classified by GO and pathway according to their function. In addition, some gene sets obtained by hierarchical cluster analysis were also categorized by GO. Enrichment factors for each GO and pathway were defined as (nf/n)/(Nf/N), where nf is the number of flagged genes within the category, Nf is the total number of genes within that same category, n is the number of flagged genes on the entire microarray, and N is the total number of genes on the microarray. Statistical analysis was performed using Fisher's exact test based on a hypergeometric distribution to calculate P values. The categories with a high enrichment factor and $P<0.05$ were extracted.

Quantitative RT-PCR

Total RNA (1 μg) for each sample was used as a template to synthesize cDNA using M-MLV reverse transcriptase (Invitrogen Co., Carlsbad, CA, USA) according to the manufacturer's instructions. Quantitative Real-Time PCR (RT-PCR) was performed with SYBR Green Real-Time PCR Master Mix (Toyobo Co., Ltd., Osaka Japan., Thunderbird) in an Mx3000P (Agilent Technologies) with an initial hold step (95°C for 60 seconds) and 40 cycles of a two-step PCR (95°C for 15 seconds and 60°C for 60 seconds). At each cycle, the fluorescence intensity of each sample was measured to monitor amplification of the target gene. Relative expression levels of target genes were calculated for each sample after normalization against glyceraldehyde-3-phosphate dehydrogenase (*Gapdh*). We found no significant differences in the *Gapdh* expression between groups (data not shown). The primer sequences are shown in Table 1.

Statistical Analysis

We used 31 independent litters from 16 different rearing cages (standard rearing environment [7 independent cages] or environmental enrichment [9 independent cages]) during the perinatal period. Independent litters were composed of one pup from each dam from the control or environmental enrichment groups. The statistics were performed with the independent litter as the statistical unit. Values for body weight, food intake, immunohistochemistry, and quantitative RT-PCR are presented as the mean ± standard deviation (S.D.) One-way analysis of variance (ANOVA) followed by a subsequent simple-effects analysis with Tukey-Kramer multiple comparison test were used to determine differences between the different groups for food intake. Two-way ANOVA was used to evaluate DE exposure and rearing environment interaction effects for dependent variables. A significant interaction was interpreted by a subsequent simple-effects analysis with Tukey-Kramer multiple comparison test for quantitative RT-PCR data. An unpaired *t*-test was used for body weight and immunohistochemical analysis to detect differences between the different groups. Significance was determined at $P<0.05$.

Results

Characterization of DE

The diameter distribution of DEP in the DE chamber showed peaks at 90 nm (Figure 2A). The average number concentration of the DEP was approximately $(8.1\pm1.0)\times10^4$ (numbers/cm^3). The average concentration of exhaust constituents was maintained at 90 μg/m^3 [2.09 ppm for carbon monoxide (CO), 0.132 ppm for nitrogen dioxide (NO_2), and less than 3.62×10^{-3} ppm for sulfur dioxide (SO_2)] (Figure 2B).

Effects of Early Environmental Enrichment on Dam and her Pups

We analyzed for FosB expression in the medial preoptic area, a part of the anterior hypothalamus of the dam at weaning. The number of FosB-positive neurons in the medial preoptic area of dam reared in environmental enrichment was significantly

Table 3. Summary of gene set enrichment analysis.

Pathway	Nf	P value	Enrichment factor	GenBank Accession	Gene symbol
RIG I LIKE RECEPTOR SIGNALING PATHWAY (KEGG)	38	<0.05	8.37	NM_021274	Cxcl10
				NM_015783	Isg15
TOLL LIKE RECEPTOR SIGNALING PATHWAY (KEGG)	49	<0.05	6.49	NM_021274	Cxcl10
				NM_133211	Tlr7
CHEMOKINE RECEPTORS BIND CHEMOKINES (REACTOME)	14	<0.01	22.72	NM_021274	Cxcl10
				NM_011331	Ccl12
INTERFERON ALPHA BETA SIGNALING (REACTOME)	39	<0.05	8.16	NM_010501	Ifit3
				NM_015783	Isg15
TOLL PATHWAY (BIOCARTA)	26	<0.05	12.23	NM_007922	Elk1
				NM_133211	Tlr7
IL4 PATHWAY (BIOCARTA)	7	<0.05	22.72	NM_010570	Irs1

Gene set enrichment analysis of the microarray results for diesel exhaust exposure vs. control identified gene sets correlated with inflammatory and immune systems. *Cxcl10* expression by microarray was confirmed by quantitative RT-PCR.
doi:10.1371/journal.pone.0070145.t003

Table 4. Functional analysis of cluster A using Gene Ontology (GO).

GO ID	Term	Nf	P value	Enrichment factor	GenBank Accession	Gene symbol
GO:0051607	defense response to virus	62	<0.001	21.21	NM_021274	Cxcl10
					NM_010501	Ifit3
					NM_011854	Oasl2
					NM_015783	Isg15
GO:0006955	immune response	62	<0.001	21.21	NM_021274	Cxcl10
					NM_011331	Ccl12
					NM_011854	Oasl2
					NM_012060	Bcap31
GO:0009615	response to virus	32	<0.001	30.82	NM_010501	Ifit3
					NM_011854	Oasl2
					NM_029803	Ifi27l2a
GO:0006954	inflammatory response	94	<0.01	10.49	NM_009793	Camk4
					NM_021274	Cxcl10
					NM_011331	Ccl12
GO:0008009	chemokine activity	14	<0.001	46.97	NM_021274	Cxcl10
					NM_011331	Ccl12
GO:0006935	chemotaxis	41	<0.01	16.04	NM_021274	Cxcl10
					NM_011331	Ccl12
GO:0005125	cytokine activity	58	<0.05	11.34	NM_021274	Cxcl10
					NM_011331	Ccl12
GO:0045087	innate immune response	97	<0.05	6.78	NM_010501	Ifit3
					NM_011854	Oasl2

The results of the gene annotation of cluster A using GO identified gene sets correlated with inflammatory and immune systems. *Cxcl10* expression by microarray was confirmed by quantitative RT-PCR.
doi:10.1371/journal.pone.0070145.t004

Table 5. Functional analysis of cluster B using Gene Ontology (GO).

GO ID	Term	Nf	P value	Enrichment factor	GenBank Accession	Gene symbol
GO:0005576	extracellular region	625	<0.001	6.95	NM_001037939	Bglap
					NM_001032298	Bglap2
					NM_013650	S100a8
					NM_177465	Umodl1
					NM_021564	Fetub
GO:0005615	extracellular space	335	<0.001	12.97	NM_001102405	Acp5
					NM_001032298	Bglap2
					NM_013650	S100a8
					NM_177465	Umodl1
					NM_021564	Fetub
GO:0005509	calcium ion binding	343	<0.001	10.13	NM_001037939	Bglap
					NM_001032298	Bglap2
					NM_013650	S100a8
					NM_177465	Umodl1

The results of the gene annotation of cluster B using GO identified gene sets correlated with abovementioned GO terms. *Umodl1* expression by microarray was confirmed by quantitative RT-PCR.
doi:10.1371/journal.pone.0070145.t005

decreased compared with that of dam reared in a standard laboratory cage environment (Figure S2A–D). Eye opening of pups, observed at postnatal day 13 or 14, was accelerated by environmental enrichment during the perinatal period (Figure S3A). Food intake per cage (one dam and 8 pups) was significantly increased during the final lactation period (postnatal days 21–25) by environmental enrichment (Figure S3B).

Effects of Exposure to Diesel Exhaust on the Lung

Body weight gain of control and enriched mice was similar to that of those exposed to DE (Figure S1D). We evaluated the histology of the lung of mice to confirm the induced toxicity under conditions of the present experimental design of diesel exhaust exposure. There was no remarkable difference in pathological finding among DE exposure groups (C-DE, EE-DE) and non-exposure groups (C-C, EE-C). Macrophages that phagocytized DEP were slightly observed in the bronchiolar lumen of mice after exposure to DE (C-DE, EE-DE) (Figure S4A–D).

Profiling and Visualization of Gene Expression Pattern by cDNA Microarray and Hierarchical Clustering Analysis

The effects of DE exposure and rearing environment during the perinatal period on the gene expression pattern in the olfactory bulb were evaluated by microarray. From the 62,976 spots (28,620 genes) printed on the microarray, 18,190 spots (15,332 genes) were found with GenBank accession numbers and a high-quality signal. Moreover, 116 spots (112 genes) were found to be differentially expressed (1.5-fold upregulated or downregulated) either in C-DE/C-C, EE-DE/EE-C, or EE-DE/C-C comparisons (Table S1), but surprisingly, there were no gene differences between the C-C and EE-C groups. Hierarchical clustering analysis classified the 116 spots into three major clusters based on their expression patterns. We showed the combined effect of diesel exhaust exposure and rearing environment by EE-DE/C-C comparison in the heat map. The combined impact cannot be visualized by only C-DE/C-C and EE-DE/EE-C comparisons. The gene expression patterns in cluster A (43 genes) and cluster C (47 genes) were upregulated and downregulated in either C-DE/C-C or EE-DE/EE-C comparisons, respectively. The gene expression pattern in cluster B (17 genes) exhibited a different expression change between C-DE/C-C and EE-DE/EE-C comparisons. This heat map allowed us to determine how these genes were related to the effects of DE exposure with or without early environmental enrichment (Figure 3).

Validation of Microarray Results by RT-PCR

We conducted RT-PCR quantification of the expression of 11 selected genes in a second set of samples (not included in the microarray experiments) to validate the microarray data and obtain expression data for each sample. All PCR reactions had efficiencies greater than 90%. From the 11 selected genes, except for *Fam13c*, RT-PCR analysis validated the results for 10 genes: *Chmp4b*, *Cxcl10* and *Dbp* in cluster A (Figure 4A–D), *Cyp2f2*, *Aqp3*, *Mslnl*, *Krt18* and *Umodl1* in cluster B (Figure 5A–E), and *Nr1i3* and *Sdad1* in cluster C (Figure 6A, B). Interestingly, there was no difference in gene expression levels between EE-C and EE-DE, whereas expression levels of the genes were dysregulated by DE exposure of mice reared in a standard cage environment. As shown in Figure 4, for *Chmp4b*, two-way ANOVA showed significant main effect for DE exposure [$F(1, 27) = 4.57$, $P<0.05$] without DE exposure/rearing environment interaction; for *Cxcl10*, two-way ANOVA showed significant main effect for DE exposure [$F(1, 27) = 16.34$, $P<0.001$] without DE exposure/rearing environment interaction; for *Fam13c*, two-way ANOVA failed to find a significant main effect of DE exposure; and for *Dbp*, two-way ANOVA showed significant main effect for DE exposure [$F(1, 27) = 18.35$, $P<0.001$] without DE exposure/rearing environment interaction. As shown in Figure 5, for *Cyp2f2*, two-way ANOVA showed significant main effect for rearing environment [$F(1, 27) = 4.73$, $P<0.001$] with significant DE exposure/rearing environment interaction [$F(1, 27) = 9.19$, $P<0.01$]; for *Aqp3*, two-way ANOVA showed significant main effect for rearing environment [$F(1, 27) = 4.58$, $P<0.05$] with significant DE exposure/rearing environment interaction [$F(1, 27) = 6.23$, $P<0.05$]; for *Mslnl*, two-way ANOVA showed significant main effect for rearing environment [$F(1, 27) = 6.61$, $P<0.05$] with significant DE exposure/rearing environment interaction [$F(1, 27) = 8.67$, $P<0.01$]; for *Krt18*, two-way ANOVA showed no significant main effect for DE exposure and rearing environment with significant DE exposure/rearing environment interaction [$F(1, 27) = 8.39$, $P<0.01$]; and for *Umodl1*, two-way ANOVA showed no significant main effect for DE exposure and rearing environment with significant DE exposure/rearing environment interaction [$F(1, 27) = 11.37$, $P<0.01$]. As shown in Figure 6, for *Nr1i3*, two-way ANOVA showed significant main effect for DE exposure [$F(1, 27) = 19.87$, $P<0.001$] with significant DE exposure/rearing environment interaction [$F(1, 27) = 6.93$, $P<0.05$], and for *Sdad1*, two-way ANOVA showed significant main effect for DE exposure [$F(1, 27) = 6.05$, $P<0.05$] without a DE exposure/rearing environment interaction.

Functional Classification of Microarray Data

Functional analysis using GO revealed that 112 genes (on the 116 spots) were enriched in nine potentially important categories with both a high enrichment factor (≥5) and statistical significance ($P<0.05$). The largest group of the functional categories was those related to immune and inflammation modulation. In particular, "inflammatory response" and "innate immune response" were included in the largest number of dysregulated genes (five genes), together with "immune response" (four genes), "chemotaxis" (three genes), and "chemokine activity" (two genes). Other interesting categories were "defense response to virus" (five genes), "response to virus" (three genes), and "sensory perception of

Table 6. Functional analysis of cluster C using Gene Ontology (GO).

GO ID	Term	Nf	P value	Enrichment factor	GenBank Accession	Gene symbol
GO:0045087	innate immune response	97	<0.05	7.84	NM_001170333	Clec4a2
					NM_133211	Tlr7

The results of the gene annotation of cluster C using GO identified gene sets correlated with inflammatory and immune systems.
doi:10.1371/journal.pone.0070145.t006

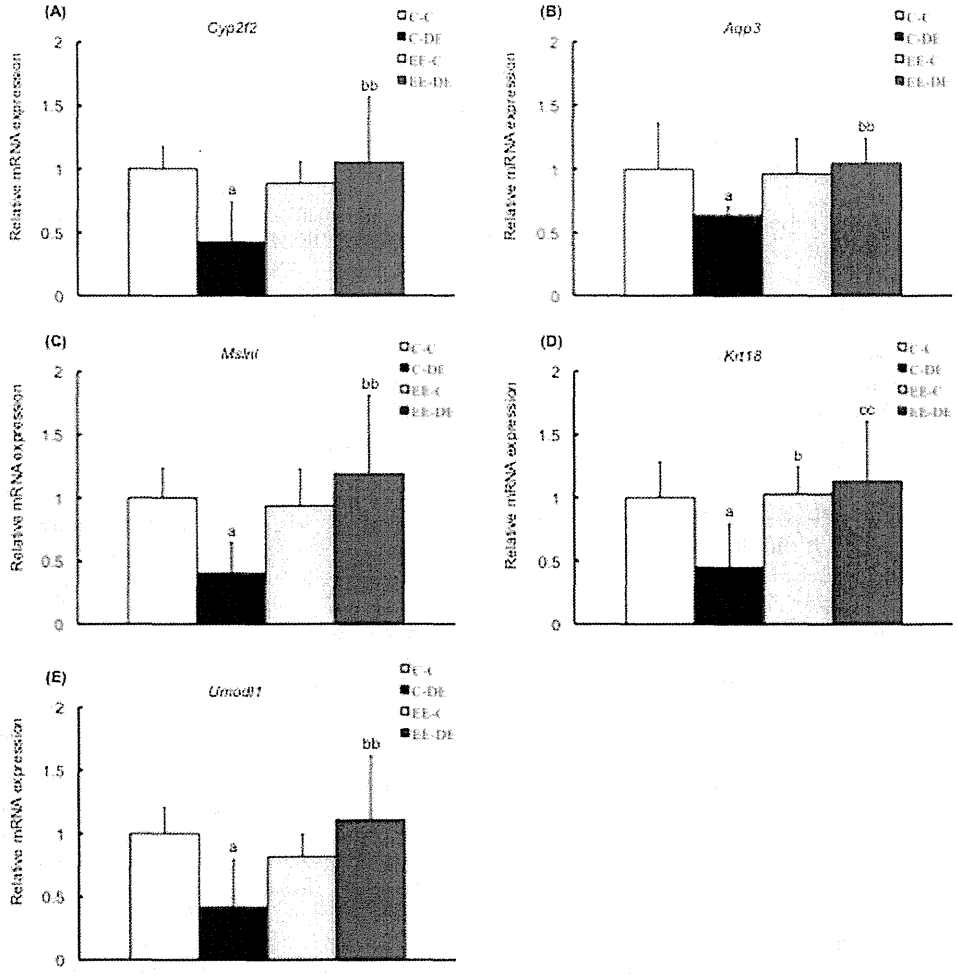

Figure 5. Confirmation of microarray data in cluster B by RT-PCR. Data show mRNA expressions for (A) *Cyp2f2*, (B) *Aqp3*, (C) *Mslnl*, (D) *Krt18*, and (E) *Umodl1* in the olfactory bulb of mice in each group. *Cyp2f2*, *Aqp3*, *Mslnl*, *Krt18*, and *Umodl1* of mice reared in a standard cage environment were significantly downregulated by exposure to diesel exhaust. There was no significant effect of exposure to diesel exhaust on gene expression of mice reared in environmental enrichment. The data are expressed as relative target gene expression compared with *Gapdh* expression. Each column represents the mean ± standard deviation (C-C: n = 7, C-DE: n = 7, EE-C: n = 8, EE-DE: n = 9). Data were analyzed by two-way analysis of variance as described in the Methods section. An analysis of simple effects is as follows: *Cyp2f2*: a indicates significant differences (Tukey-Kramer method, $^{a}P<0.05$, C-C vs. C-DE); b indicates significant differences (Tukey–Kramer method, $^{bb}P<0.01$, C-DE vs. EE-DE); *Aqp3*: a indicates significant differences (Tukey–Kramer method, $^{a}P<0.05$, C-C vs. C-DE); b indicates significant differences (Tukey-Kramer method, $^{b}P<0.05$, C-DE vs. EE-DE); *Mslnl*: a indicates significant differences (Tukey–Kramer method, $^{a}P<0.05$, C-C vs. C-DE); b indicates significant differences (Tukey–Kramer method, $^{bb}P<0.01$, C-DE vs. EE-DE); *Krt18*: a indicates significant differences (Tukey–Kramer method, $^{a}P<0.05$, C-C vs. C-DE); b indicates significant differences (Tukey-Kramer method, $^{b}P<0.05$, C-DE vs. EE-C); c indicates significant differences (Tukey–Kramer method, $^{cc}P<0.01$, C-DE vs. EE-DE); *Umodl1*: a indicates significant differences (Tukey–Kramer method, $^{a}P<0.05$, C-C vs. C-DE); and b indicates significant differences (Tukey–Kramer method, $^{bb}P<0.01$, C-DE vs. EE-DE).
doi:10.1371/journal.pone.0070145.g005

smell" (three genes) (Table 2). Six pathways were also identified from the 112 genes data (Table 3). Biological pathway analysis incriminated related pathways, which were modulated by DE exposure. Several immune-related pathways, including "RIG-I-like receptor signaling pathway", "Toll-like receptor signaling pathway", "Chemokine receptors bind chemokines", "Interferon alpha beta signaling", "Toll pathway", and "IL4 pathway" were significantly overrepresented. The results of the GO analysis showed that the genes in clusters A, B and C were enriched in eight (Table 4), three (Table 5) and one (Table 6) potentially important categories, respectively. Six genes in cluster A, three genes in cluster B, and 15 genes in cluster C were not annotated to any GO.

Discussion

There is increasing evidence that DE inhalation may result in neurotoxicity [13,14,34], but the effect of a low concentration of subacute DE exposure on the central nervous system is poorly understood. The present study provides experimental evidence that 28-day DE exposure at an environmental concentration dysregulated gene expression in the olfactory bulb of mice reared in a standard cage environment. In addition, we demonstrated that environmental enrichment during the perinatal period reversed the results of gene expression in the olfactory bulb induced by DE inhalation. The results of the present study indicate for the first time that the effect of DE exposure on gene expression

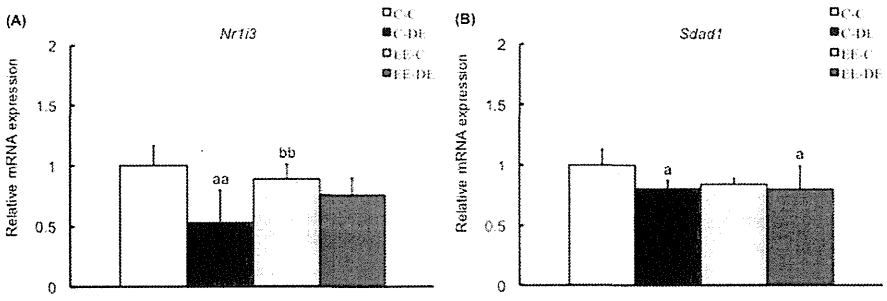

Figure 6. Confirmation of microarray data in cluster C by RT-PCR. Data show mRNA expressions for (A) *Nr1i3*, and (B) *Sdad1* in the olfactory bulb of mice in each group. *Nr1i3* and *Sdad1* of the olfactory bulb of mice reared in a standard cage environment were significantly downregulated by exposure to diesel exhaust. There was no significant effect of exposure to diesel exhaust on gene expressions of mice reared in environmental enrichment. The data are expressed as relative target gene expression compared with *Gapdh* expression. Each column represents the mean ± standard deviation (C-C: n = 7, C-DE: n = 7, EE-C: n = 8, EE-DE: n = 9). Data were analyzed by two-way analysis of variance as described in the Methods section. An analysis of simple effects is as follows: *Nr1i3*: a indicates significant differences (Tukey–Kramer method, $^{aa}P<0.01$, C-C vs. C-DE); b indicates significant differences (Tukey–Kramer method, $^{bb}P<0.01$, C-DE vs. EE-C); and *Sdad1*: a indicates significant differences (Tukey–Kramer method, $^{a}P<0.05$, C-C vs. C-DE and C-C vs. EE-DE).
doi:10.1371/journal.pone.0070145.g006

patterns was influenced by rearing environment during the perinatal period.

First, we characterized particle size distribution and mass concentration of DEP. We produced a mass concentration of DEP at 90 $\mu g/m^3$, which is environmentally relevant. This approach using a DE inhalation chamber is more relevant to human exposure scenarios than other methods of exposure, such as nasal drop, oral or intratracheal DEP administration. There is an emerging concern about the effects of suspended PM in air pollutants mainly derived from DEP [6]. Numerous urban areas in the world demonstrate PM concentrations of 200 to 600 $\mu g/m^3$ in annual averages and frequently exceeding a peak concentration of 1,000 $\mu g/m^3$ [35]. Under the worst conditions in the United States and assuming a ventilation rate of 6 L/minute (8.6 m^3/day) for a healthy adult at rest, the total amount of PM exposure would be 4,600 μg. This would correspond to approximately 40 μg/day of PM exposure for a mouse with a ventilation rate of 35–50 mL/minute [36]. The DE exposure in this study was approximately 2.2 μg/day. In the present study, the DE exposure condition for DEP mass concentration and exposure time was designed to be lower than comparative recent experimental studies on the effect of inhalation exposure to DE on the central nervous system [13,14,37,38,39,40].

Our microarray data showed that exposure to a low concentration of DE changed expression of 112 genes in the olfactory bulb of mice (Table S1). Moreover, quantitative RT-PCR analysis confirmed 10 genes from the microarray data. The results suggested that two replicates of the pooled sample detected unreliable data with relatively low signal intensity and improved measurement precision. It was reported that fold change analysis alone is an unreliable indicator [41,42]. Several publications have made specific recommendations on the number of replicates required to detect dysregulated genes based on fold change criteria [43,44]. The major advantage of this approach was that averaging across replicates increased the precision of gene expression measurements and allowed smaller changes to be detected. In fact, in the present study, the quantitative RT-PCR analysis results supported the accuracy of the microarray data.

Second, we investigated by cDNA microarray how rearing environment during the perinatal period altered the effects of DE exposure on gene expression in the olfactory bulb. GO and pathway analysis were conducted to obtain biological and functional analysis from the microarray data. GO terms and pathways related to immune and inflammation responses were largely extracted from the data of 112 genes. These results suggested that a low concentration exposure to DE affected the expression of genes involved in immune and inflammatory responses in the olfactory bulb. These results are consistent with data from previous studies indicating that DE and DEP triggered oxidative stress and inflammation in brain tissue [12,13,14,45].

To further investigate the biological and functional meanings of microarray data, we conducted hierarchical clustering to classify gene expression patterns in each group. The gene expression patterns in cluster A and cluster C were upregulated and downregulated in either C-DE/C-C or EE-DE/EE-C comparisons, respectively. In addition, quantitative RT-PCR analysis revealed a main effect of exposure to DE on the expression of genes in cluster A and cluster C without a DE exposure/environmental enrichment interaction. These results suggested that changes in the gene expression pattern in cluster A and cluster C could be attributed to the effect of DE exposure. We also demonstrated that functional analysis of cluster A using gene annotation with GO obtained a higher enrichment factor of each category involved in immune/inflammatory responses and response to virus than that of all dysregulated genes. This observation suggested that cluster A functionalized categories related to immune/inflammatory responses and response to virus compared with the genes dysregulated by DE exposure. In contrast, a subset of genes in cluster B exhibited a different expression change between C-DE/C-C and EE-DE/EE-C comparisons. In addition, quantitative RT-PCR analysis revealed a main effect of rearing environment on gene expression in cluster B with a significant DE exposure/rearing environment interaction. These results suggested that cluster B could be associated with an interaction between early rearing environment and DE exposure. Cluster B contained categories that did not include genes to immune and inflammatory responses. These results suggested that cluster B might enrich some new functional outputs by both early rearing environment and DE exposure. Therefore, the present study suggested that categorizing patterns of gene expression could identify multiple factors contributing to changes in gene expression patterns. In addition, 15 genes, such as *Sdad1*, were not annotated to any GO in cluster C. Hierarchical cluster analysis categorized actual gene expression patterns, which could be used to infer

functional roles for unknown genes in cluster C. However, it is notable that cluster analysis does not give absolute answers, although there are data-mining techniques that allow relationships in the data to be explored. Further investigation will be needed to investigate a function and localization *in situ* of genes that were not annotated to any GO.

Finally, quantitative RT-PCR analysis revealed that DE exposure dysregulated gene expression levels in the olfactory bulb of mice reared in a standard cage environment, whereas no difference between control and DE-exposed mice reared in conditions of environmental enrichment was detected (Figures 4, 5, 6). These results suggested that early rearing environment might influence the effects of DE exposure. Early rearing environment, in particular, mother-infant interaction is essential for brain development. The medial preoptic area of the hypothalamus is a critical region for the expression of maternal behavior in rodents, and neurons in the medial preoptic area are active during maternal behavior as demonstrated by immunohistochemical analysis of FosB [46,47]. Expression of FosB in the medial preoptic area of dams has been shown to be necessary for nurturing [48,49]. The present study showed that expression levels of FosB in the medial preoptic area of dams reared in environmental enrichment significantly decreased compared with that of dams reared in a standard cage environment at weaning (Figure S2A–D). In addition, the present study also showed that pups reared in environmental enrichment during the perinatal period accelerated eye opening (Figure S3A) and increased feeding at postnatal days 21–25 (Figure S3B), suggesting that early environmental enrichment could promote pup development because of possible changes in the interactions between mother and pups, which was consistent with results from a previous study [50]. Perinatal environmental stress can have persistent effects on the mother, which may influence maternal behavior. In rodents, repeated daily restraint, lack of environmental enrichment, during the perinatal period decreased maternal care to the pups [51]. Because adoption reverses the negative effects of perinatal stress on hypothalamic-pituitary-adrenal axis function, it was hypothesized that disturbance of the mother-infant interaction may cause stress on the offspring and contribute to the long-term effects of perinatal stress. Similar mechanisms are suspected for the immune alterations observed in perinatally stressed animals [52]. Mother–infant interactions were also regulated by the olfactory system [53]. It has been reported that early environmental stress affected the magnitude of maternal behavior and nest odor preference modulated by the olfactory bulb in pups [54]. Aggressive behavior and olfactory bulb structure were altered by the laboratory cage environment [55]. Dysfunction of the olfactory bulb leads to numerous immune changes, such as reduced neutrophil phagocytosis, lymphocyte mitogenesis, lymphocyte number and negative acute phase proteins, increased leukocyte adhesiveness/aggregation, monocyte phagocytosis, neutrophil number and positive acute phase proteins [56]. It has been reported that activation of the inflammatory system in olfactory dysfunction changes immune response to further immune challenges [57]. However, little is known whether early rearing environment exacerbates the effects of exposure to DE on the central nervous system. Critical developmental windows of vulnerability of the immune system to environmental programming are presently unknown, but the present study showed that effects of exposure to DE on gene expression involved in the immune system in the olfactory bulb were dependent on the rearing environment.

Previous studies have reported the early environmental origins of neurodegenerative disease in later life [58]. Mice housed in a standard laboratory cage setting exhibited higher rates of stereotypical behaviors at early development [15] than those of mice in environmental enrichment conditions [17]. These findings suggest the importance of environmental factors, such as rearing environment during the perinatal period in investigational neurotoxicology studies. We focused on the olfactory bulb because the olfactory bulb is important for the maintenance of psychiatric illnesses, such as depression [57]. The present study showed for the first time that rearing environment during the perinatal period influenced the effects of DE exposure on the olfactory bulb. The International Agency for Research on Cancer concluded that DE is carcinogenic to humans (Group 1) in 2012, although recently DEP concentrations in the environment have been significantly decreased. However, there is little evidence of the effects of exposure to DE at environmental concentrations on the central nervous system. We have just begun to observe the effect of low concentrations of DE on the central nervous system. Our findings suggest that the influence on the developing brain of housing environment, such as environmental enrichment in early life, might be an important contributor to the effects of previously unidentified toxic environmental agents, such as DE.

In conclusion, our study demonstrates that DE-induced dysregulated genes of the olfactory bulb were influenced by early housing environment. We reported that 28-day DE exposure affected immune and inflammatory responses when reared in a standard cage environment during the perinatal period, but not when reared in environmental enrichment during this same period. These results provide novel insights regarding housing environment for the evaluation of health effects of DE. Further investigation is required to investigate the precise mechanisms of immune response and histological analyses of environmental concentrations of DE on olfactory bulb of mice reared in different housing environments.

Supporting Information

Figure S1 Body weight. There was no difference in body weight between mice in control and environmental enrichment groups (Unpaired *t*-test). The data are expressed as a mean of the value of body weight in the control dam and environmental enrichment dam at (A) gestational day 14 (n = 9) and (B) weaning (n = 9). The data are expressed as a mean of the value of body weight (C) in control pups and environmental enrichment pups at postnatal (P) days 10 and 26 (n = 10). (D) The data are expressed as a mean of the value of the changed body weight in male offspring by 28-day diesel exhaust inhalation (C-C: n = 7, C-DE: n = 7, EE-C: n = 8, EE-DE: n = 9). Each column represents the mean ± standard deviation.
(TIFF)

Figure S2 Data by immunohistochemical analysis show FosB expression in the medial preoptic area of the hypothalamus of dam at weaning. Images show a representation of the immunostaining procedure that labeled FosB as black [(A) Control, (B) Environmental enrichment]. Scale bar = 100 μm. (C) Mean (± standard deviation) numbers of FosB-positive cells in the medial preoptic area of the hypothalamus: flesh color indicated in (D) of control and environmental enrichment dam (n = 3). Environmental enrichment decreased FosB-positive cells in the medial preoptic area of the hypothalamus (Unpaired *t*-test, $^{**}P<0.01$).
(TIFF)

Figure S3 Effect of environmental enrichment during the perinatal period on pup development. (A) Environmental enrichment during the perinatal period increased food intake. A dam and her pups (n = 7–9 per cage) in a home cage were

considered to be one cage (N = 1). The graph shows the mean food intake of white circles (control cage; N = 8) and black squares (environmental enrichment cage; N = 9) for each age. On postnatal (P) days 21–25, environmental enrichment increased food intake (Tukey–Kramer method, **P<0.01.). Values are mean ± standard deviation. (B) Precocious eye opening in environmentally enriched mice. The percentage of postnatal (P) day 13 (white column) and P 14 (black column) pups that opened their eyes in the indicated cages is shown.
(TIFF)

Figure S4 Effect of exposure to diesel exhaust on lung tissue. Images show a representation of histology of lung by exposure to clean air [(A): C-C, (C): EE-C] or diesel exhaust [(B): C-DE, (D): EE-DE]. Scale bar = 20 μm. (B, D) Macrophages that phagocytized diesel exhaust particles were observed in the bronchiolar lumen of mice (arrow). However, there was no difference in pathological findings among groups.
(TIFF)

Table S1 List of significantly expressed genes.
(DOC)

Acknowledgments

We thank Dr. Yusuke Shinkai, Mr. Shotaro Matsuzawa, Mr. Keisuke Sekita, Mrs. Hiroko Ochiai, and Mr. Ryo Uzuki (Department of Hygienic Chemistry, Faculty of Pharmaceutical Sciences, Tokyo University of Science) for their assistance in maintaining diesel exhaust exposure and tissue sampling.

Author Contributions

Conceived and designed the experiments: S. Yokota. Performed the experiments: S. Yokota HH RN. Analyzed the data: S. Yokota HH MU. Contributed reagents/materials/analysis tools: S. Yokota HH MU NK RN S. Yanagita. Wrote the paper: S. Yokota. Project leader: KT. Interpretation of the results: S. Yokota KT.

References

1. Wichmann HE (2007) Diesel exhaust particles. Inhal Toxicol 19 Suppl 1: 241–244.
2. McClellan RO (1987) Health effects of exposure to diesel exhaust particles. Annu Rev Pharmacol Toxicol 27: 279–300.
3. Muranaka M, Suzuki S, Koizumi K, Takafuji S, Miyamoto T, et al. (1986) Adjuvant activity of diesel-exhaust particulates for the production of IgE antibody in mice. J Allergy Clin Immunol 77: 616–623.
4. Sagai M, Furuyama A, Ichinose T (1996) Biological effects of diesel exhaust particles (DEP). III. Pathogenesis of asthma like symptoms in mice. Free Radic Biol Med 21: 199–209.
5. Silverman DT, Samanic CM, Lubin JH, Blair AE, Stewart PA, et al. (2012) The Diesel Exhaust in Miners study: a nested case-control study of lung cancer and diesel exhaust. J Natl Cancer Inst 104: 855–868.
6. Donaldson K, Tran L, Jimenez LA, Duffin R, Newby DE, et al. (2005) Combustion-derived nanoparticles: a review of their toxicology following inhalation exposure. Part Fibre Toxicol 2: 10.
7. Elder A, Gelein R, Silva V, Feikert T, Opanashuk L, et al. (2006) Translocation of inhaled ultrafine manganese oxide particles to the central nervous system. Environ Health Perspect 114: 1172–1178.
8. Oberdörster G, Sharp Z, Atudorei V, Elder A, Gelein R, et al. (2004) Translocation of inhaled ultrafine particles to the brain. Inhal Toxicol 16: 437–445.
9. Oberdörster G, Oberdörster E, Oberdörster J (2005) Nanotoxicology: an emerging discipline evolving from studies of ultrafine particles. Environ Health Perspect 113: 823–839.
10. Peters A, Veronesi B, Calderón-Garcidueñas L, Gehr P, Chen LC, et al. (2006) Translocation and potential neurological effects of fine and ultrafine particles a critical update. Part Fibre Toxicol 3: 13.
11. Block ML, Wu X, Pei Z, Li G, Wang T, et al. (2004) Nanometer size diesel exhaust particles are selectively toxic to dopaminergic neurons: the role of microglia, phagocytosis, and NADPH oxidase. FASEB J 8: 1618–1620.
12. Hartz AM, Bauer B, Block ML, Hong JS, Miller DS (2008) Diesel exhaust particles induce oxidative stress, proinflammatory signaling, and P-glycoprotein up-regulation at the blood-brain barrier. FASEB J 22: 2723–2733.
13. Levesque S, Surace MJ, McDonald J, Block ML (2011) Air pollution & the brain: Subchronic diesel exhaust exposure causes neuroinflammation and elevates early markers of neurodegenerative disease. J Neuroinflammation 8: 105.
14. Levesque S, Taetzsch T, Lull ME, Kodavanti U, Stadler K, et al. (2011) Diesel exhaust activates and primes microglia: air pollution, neuroinflammation, and regulation of dopaminergic neurotoxicity. Environ Health Perspect 119: 1149–1155.
15. Powell SB, Newman HA, Pendergast JF, Lewis MH (1999) A rodent model of spontaneous stereotypy: initial characterization of developmental, environmental, and neurobiological factors. Physiol Behav 66: 355–363.
16. Benefiel AC, Greenough PhD WT (1998) Effects of Experience and Environment on the Developing and Mature Brain: Implications for Laboratory Animal Housing. ILAR J 39: 5–11.
17. Turner CA, Lewis MH (2003) Environmental enrichment: effects on stereotyped behavior and neurotrophin levels. Physiol Behav 80: 259–266.
18. Lewis MH, Tanimura Y, Lee LW, Bodfish JW (2007) Animal models of restricted repetitive behavior in autism. Behav Brain Res 176: 66–74.
19. Berkson G (1983) Repetitive stereotyped behaviors. Am J Ment Defic 88: 239–246.
20. Lewis MH, Bodfish JW, Powell SB, Parker DE, Golden RN (1996) Clomipramine treatment for self-injurious behavior of individuals with mental retardation: a double-blind comparison with placebo. Am J Ment Retard 100: 654–665.
21. Lewis MH, Bodfish JW, Powell SB, Wiest K, Darling M, et al. (1996) Plasma HVA in adults with mental retardation and stereotyped behavior: biochemical evidence for a dopamine deficiency model. Am J Ment Retard 100: 413–418.
22. Garner JP (2005) Stereotypies and other abnormal repetitive behaviors: potential impact on validity, reliability, and replicability of scientific outcomes. ILAR J 46: 106–117.
23. Dean SW (1999) Environmental enrichment of laboratory animals used in regulatory toxicology studies. Lab Anim 33: 309–327.
24. Lewis MH (2004) Environmental complexity and central nervous system development and function. Ment Retard Dev Disabil Res Rev 10: 91–95.
25. Matsui Y, Sakai N, Tsuda A, Terada Y, Takaoka M, et al. (2009) Spectrochimica Acta Part B 64: 796–801.
26. Kilkenny C, Browne W, Cuthill IC, Emerson M, Altman DG (2010) Animal research: reporting in vivo experiments: the ARRIVE guidelines. Br J Pharmacol 160: 1577–1579.
27. Callahan TA, Piekut DT (1997) Differential Fos expression induced by IL-1beta and IL-6 in rat hypothalamus and pituitary gland. J Neuroimmunol 73: 207–211.
28. Serino R, Ueta Y, Hara Y, Nomura M, Yamamoto Y, et al. (1999) Centrally administered adrenomedullin increases plasma oxytocin level with induction of c-fos messenger ribonucleic acid in the paraventricular and supraoptic nuclei of the rat. Endocrinology 140: 2334–2342.
29. Brazma A, Hingamp P, Quackenbush J, Sherlock G, Spellman P, et al. (2001) Minimum information about a microarray experiment (MIAME)-toward standards for microarray data. Nat Genet 29: 365–371.
30. Zahurak M, Parmigiani G, Yu W, Scharpf RB, Berman D, et al. (2007) Preprocessing Agilent microarray data. BMC Bioinformatics 8: 142.
31. Quackenbush J (2001) Computational analysis of microarray data. Nat Rev Genet 2: 418–427.
32. Eisen MB, Spellman PT, Brown PO, Botstein D (1998) Cluster analysis and display of genome-wide expression patterns. Proc Natl Acad Sci U S A 95: 14863–14868.
33. Saldanha AJ (2004) Java Treeview–extensible visualization of microarray data. Bioinformatics 20: 3246–3248.
34. Yokota S, Mizuo K, Moriya N, Oshio S, Sugawara I, et al. (2009) Effect of prenatal exposure to diesel exhaust on dopaminergic system in mice. Neurosci Lett 449: 38–41.
35. UN Environment Program and WHO Report (1994) Air Pollution in the world's megacities. A Report from the U.N. Environment Programme and WHO. Environment 36: 5–37.
36. de Hennezel L, Debarre S, Ramisse F, Delamanche S, Harf A, et al. (2001) Plethysmography for the assessment of pneumococcal pneumonia and passive immunotherapy in a mouse model. Eur Respir J 17: 94–99.
37. Yamagishi N, Ito Y, Ramdhan DH, Yanagiba Y, Hayashi Y, et al. (2012) Effect of nanoparticle-rich diesel exhaust on testicular and hippocampus steroidogenesis in male rats. Inhal Toxicol 24: 459–467.
38. Win-Shwe TT, Fujimaki H, Fujitani Y, Hirano S (2012) Novel object recognition ability in female mice following exposure to nanoparticle-rich diesel exhaust. Toxicol Appl Pharmacol 262: 355–362.
39. Jacob A, Hartz AM, Potin S, Coumoul X, Yousif S, et al. (2011) Aryl hydrocarbon receptor-dependent upregulation of Cyp1b1 by TCDD and diesel exhaust particles in rat brain microvessels. Fluids Barriers CNS 8: 23.
40. Win-Shwe TT, Yamamoto S, Fujitani Y, Hirano S, Fujimaki H (2012) Nanoparticle-rich diesel exhaust affects hippocampal-dependent spatial learning

and NMDA receptor subunit expression in female mice. Nanotoxicology 6: 543–553.
41. Chen Y, Dougherty ER, Bittner ML (1997) Ratio-based decisions and the quantitative analysis of cDNA microarray images. J Biomed Opt 2: 364–374.
42. Newton MA, Kendziorski CM, Richmond CS, Blattner FR, Tsui KW (2001) On differential variability of expression ratios: improving statistical inference about gene expression changes from microarray data. J Comput Biol 8: 37–52.
43. Pan W, Lin J, Le CT (2002) How many replicates of arrays are required to detect gene expression changes in microarray experiments? A mixture model approach. Genome Biol 3(5): research0022.
44. Tibshirani R (2006) A simple method for assessing sample sizes in microarray experiments. BMC Bioinformatics 7: 106.
45. Gerlofs-Nijland ME, van Berlo D, Cassee FR, Schins RP, Wang K. et al. (2010) Effect of prolonged exposure to diesel engine exhaust on proinflammatory markers in different regions of the rat brain. Part Fibre Toxicol 7: 12.
46. Numan M, Numan MJ, Marzella SR, Palumbo A (1998) Expression of c-fos, fos B, and egr-1 in the medial preoptic area and bed nucleus of the stria terminalis during maternal behavior in rats. Brain Res 792: 348–352.
47. Stack EC, Numan M (2000) The temporal course of expression of c-Fos and Fos B within the medial preoptic area and other brain regions of postpartum female rats during prolonged mother–young interactions. Behav Neurosci 114: 609–622.
48. Brown JR, Ye H, Bronson RT, Dikkes P, Greenberg ME (1996) A defect in nurturing in mice lacking the immediate early gene fosB. Cell 86: 297–309.
49. Kuroda KO, Meaney MJ, Uetani N, Kato T (2008) Neurobehavioral basis of the impaired nurturing in mice lacking the immediate early gene FosB. Brain Res 1211: 57–71.
50. Cancedda L, Putignano E, Sale A, Viegi A, Berardi N, et al. (2004) Acceleration of visual system development by environmental enrichment. J Neurosci 24: 4840–4848.
51. Maccari S, Piazza PV, Kabbaj M, Barbazanges A, Simon H. et al. (1995) Adoption reverses the long-term impairment in glucocorticoid feedback induced by prenatal stress. J Neurosci 15: 110–116.
52. Gorczynski RM (1992) Conditioned stress responses by pregnant and/or lactating mice reduce immune responses of their offspring after weaning. Brain Behav Immun 6: 87–95.
53. Lévy F, Keller M, Poindron P (2004) Olfactory regulation of maternal behavior in mammals. Horm Behav 46: 284–302.
54. de Souza MA, Szawka RE, Centenaro LA, Diehl LA, Lucion AB (2012) Prenatal stress produces sex differences in nest odor preference. Physiol Behav 105: 850–855.
55. Oliva AM, Salcedo E, Hellier JL, Ly X, Koka K, et al. (2010) Toward a mouse neuroethology in the laboratory environment. PLoS One 5: e11359.
56. Kelly JP, Wrynn AS, Leonard BE (1997) The olfactory bulbectomized rat as a model of depression: an update. Pharmacol Ther 74: 299–316.
57. Song C, Leonard BE (2005) The olfactory bulbectomised rat as a model of depression. Neurosci Biobehav Rev 29: 627–647.
58. Landrigan PJ, Sonawane B, Butler RN, Trasande L, Callan R, et al. (2005) Early environmental origins of neurodegenerative disease in later life. Environ Health Perspect 113: 1230–1233.

The Journal of Toxicological Sciences (J. Toxicol. Sci.)
Vol.38, No.3, 363-370, 2013

Letter

Prenatal exposure to zinc oxide particles alters monoaminergic neurotransmitter levels in the brain of mouse offspring

Yuka Okada[1,*], Ken Tachibana[1,3,*], Shinya Yanagita[2,3,4] and Ken Takeda[1,2,3]

[1]Department of Hygienic Chemistry, Faculty of Pharmaceutical Sciences, Tokyo University of Science, 2641 Yamazaki, Noda, Chiba 278-8510, Japan
[2]Research Center for Health Science of Nanoparticles, Research Institute for Science and Technology, Tokyo University of Science, 2641 Yamazaki, Noda, Chiba 278-8510, Japan
[3]The Center for Environmental Health Science for the Next Generation, Research Institute for Science and Technology, Tokyo University of Science, 2641 Yamazaki, Noda, Chiba 278-8510, Japan
[4]Faculty of Science and Technology, Tokyo University of Science, 2641 Yamazaki, Noda, Chiba 278-8510, Japan

(Received February 8, 2013; Accepted March 6, 2013)

ABSTRACT — Zinc oxide (ZnO) nano-sized particles (NPs) are beneficial materials used for sunscreens and cosmetics. Although ZnO NPs are widely used for cosmetics, the health effects of exposure during pregnancy on offspring are largely unknown. Here we investigated the effects of prenatal exposure to ZnO NPs on the monoaminergic system of the mouse brain. Subcutaneous administration of ZnO NPs to the pregnant ICR mice (total 500 μg/mouse) were carried out and then measured the levels of dopamine (DA), serotonin (5-HT), and noradrenalin, and their metabolites in 9 regions of the brain of offspring (6-week-old) using high performance liquid chromatography (HPLC). HPLC analysis demonstrated that DA levels were increased in hippocampus in the ZnO NP exposure group. In the levels of DA metabolites, homovanillic acid was increased in the prefrontal cortex and hippocampus, and 3, 4-dihydroxyphenylacetic acid was increased in the prefrontal cortex by prenatal ZnO NP exposure. Furthermore, DA turnover levels were increased in the prefrontal cortex, neostriatum, nucleus accumbens, and amygdala in the ZnO NP exposure group. We also found changes of the levels of serotonin in the hypothalamus, and of the levels of 5-HIAA (5-HT metabolite) in the prefrontal cortex and hippocampus in the ZnO NP-exposed group. The levels of 5-HT turnover were increased in each of the regions except for the cerebellum by prenatal ZnO NP exposure. The present study indicated that prenatal exposure to ZnO NPs might disrupt the monoaminergic system, and suggested the possibility of detrimental effects on the mental health of offspring.

Key words: Brain, Monoaminergic neurotransmitter, Nanoparticle, Prenatal exposure, Zinc oxide

INTRODUCTION

Nano-sized particles (NPs) are widely used for medicine, industrial products, and cosmetics (Morabito *et al.*, 2011; Kuan *et al.*, 2012). In particular, NPs of zinc oxide (ZnO) and titanium dioxide (TiO_2) are beneficial to sunscreens and foundation because these particles are colorless and reflect ultraviolet rays (Nohynek *et al.*, 2007). While the physical and chemical characteristics of NPs make them useful for many industrial applications, previous studies revealed that NPs can enter the systemic circulation, and migrate to various organs such as the liver, kidney, spleen, and heart (Kreyling *et al.*, 2009; Liu *et al.*, 2009; Oberdörster *et al.*, 2009). Some NPs induce production of inflammatory cytokines (Oberdörster, 2001; Beckett *et al.*, 2005; Tin Tin Win *et al.*, 2006), and affect the monoaminergic neurotransmitters (Tin Tin Win *et al.*, 2008). Monoaminergic neurotransmitters

Correspondence: Ken Takeda (E-mail: takedak@rs.noda.tus.ac.jp)
Ken Tachibana (E-mail: ktachiba@rs.noda.tus.ac.jp)
*These authors equally contributed to this work.

such as dopamine (DA), noradrenaline (NA), and serotonin (5-HT) play a pivotal role in several physiological and psychological functions. Several reports have suggested that monoaminergic system disruption is related to psychiatric disorders including schizophrenia, depression, autism, and attention-deficit hyperactivity disorder (Froehlich *et al.*, 2010; Nakamura *et al.*, 2010; Paclt *et al.*, 2009).

We previously demonstrated that nano-sized TiO_2, administered to pregnant mice, was transferred to the offspring and affected the reproductive and central nervous system of male offspring (Takeda *et al.*, 2009). Because a fetus is highly vulnerable to environmental stimuli, chemical exposure in the fetal period generally disrupts its development (Kawashiro *et al.*, 2008; Needham and Sexton, 2000). Although these aspects suggest that the detrimental health effects of the NPs would be more profound in fetuses than in adults, the potential toxicity of prenatal exposure of NPs is less investigated. We recently reported that prenatal exposure to TiO_2 NPs affects gene expression related to the development and function of the central nervous systems including the monoaminergic system (Shimizu, *et al.* 2009). Because ZnO NPs are also widely used in cosmetics, there is a concern with the health effects of prenatal ZnO NP exposure on offspring. Previous studies suggest that ZnO NPs induce cytotoxicity and oxidative stress in primary mouse embryonic fibroblast (Yang *et al.*, 2009) and developmental disorder in Zebrafish (Zhu *et al.*, 2008); however its health effects on offspring exposed to ZnO NPs during the fetal period are largely unknown. In the present study, we investigated the effects of prenatal exposure to ZnO NPs on the monoaminergic systems. We comprehensively examined the levels of monoamines and their metabolites in 9 regions of the brain in mice using high performance liquid chromatography (HPLC).

MATERIALS AND METHODS

ZnO particles

Mz-300 NPs, ZnO with a primary diameter of 30-40 nm, were kindly provided by Tayca Co. (Osaka, Japan). ZnO NPs were dispersed in saline containing 0.05% Tween-80, and the sample suspension was sonicated for 90 min in a bath-type sonicator immediately before administration. To minimize the heat production, the bath was filled with enough volume of water. A wide distribution of ZnO powder of different diameters was confirmed by field emission-type scanning electron microscopy. The size distribution of the ZnO NPs in the suspension was measured by dynamic light scattering using an FPAR-1000 (Otsuka Electronics Co., Ltd., Osaka, Japan). Size distribution of ZnO NPs was assessed with the CONTIN algorithm to obtain the diameter distribution of polydispersed particles from dynamic light scattering data.

Animals

Pregnant ICR mice (8-11-week-old) at gestation day (GD) 1 were purchased from SLC Co. (Shizuoka, Japan). ZnO NPs were suspended at 0.5 mg/ml, and 0.2 ml was administrated subcutaneously to the pregnant ICR mice at GD 5, 8, 11, 14, and 17 (100 μg/mouse/day: total 500 μg/mouse). Administered ZnO NPs was same as the mass dose in the previous study about the effects of prenatal TiO_2 NP exposure on dopaminergic system (Takahashi *et al.*, 2010). Control mice were treated with saline containing 0.05% Tween-80. In each group, pups were weaned on postnatal day 21. They were housed under controlled conditions with a 12 hr light/ 12 hr dark cycle and *ad libitum* access to food and water. All experiments were handled in accordance with the institutional and national guidelines for the care and use of laboratory animals. All efforts were made to minimize the number of animals used and their suffering.

HPLC analysis of neurotransmitters

Brains were removed from 6-week-old anesthetized male pups (n = 8/group). Only male mice were analyzed in this study because the neurotransmitter variations were seen during different stages of the estrous cycle in female mice (Dazzi *et al.*, 2007; Xiao and Becker, 1994). Serial coronal sections of the brain (2 mm thick) were obtained using a Rodent brain slicer (MUROMACHI KIKAI, Tokyo, Japan) and dissected to 9 regions: prefrontal cortex, neostriatum (caudate-putamen), nucleus accumbens, hippocampus, amygdala, hypothalamus, midbrain, brainstem, and cerebellum. The dissected regions were immediately frozen in liquid nitrogen and stored at -80°C until use.

Frozen brain tissue was homogenized in ice-cold perchloric acid containing 100 mM EDTA (2Na) and 100 ng isoproterenol as an internal standard. The homogenates were centrifuged at 20,000 × g for 15 min at 0°C. Supernatants were transferred to new tubes and the pellets were stored for protein assay. The pH of the supernatant was adjusted to 3.0 with 1 M sodium acetate, and stored at -80°C until use. For HPLC analysis, 10 μl of the pH-adjusted supernatant were injected into an HPLC system with electrochemical detection (EICOM Co., Kyoto, Japan). Monoamines were separated by a C18 reverse-phase column (EICOMPAK SC-5ODS, EICOM) with a mobile phase containing sodium acetate and citric